Ticagrelor combined with aspirin displays the signature of regulating the gut microbiome in consistence with improving the immuno-inflammatory response in atherosclerosis

Zhixia Bai[1,2#], Qinning Zhang[2#], Yajuan Liu[1,2#], Yang Zhao[3], Ru Yan[1], Libo Yang[1], Huiyan Ma[2], Yi Ren[2], Ting Wang[4], Yiwei Li[4], Yuanyuan Liu[4], Xin Jiang[2], Rui Wang[1], Shaobin Jia[1*], Xiaoxia Zhang[6*], Hao Wang[5*]

1. Heart Centre & Department of Cardiovascular Diseases, General Hospital of Ningxia Medical University, Yinchuan, 750000, Ningxia, China

2. Clinical Medical College, Ningxia Medical University, Yinchuan, 750000, Ningxia, China

3. Department of Surgical Oncology II, General Hospital of Ningxia Medical University, Yinchuan, 750000, Ningxia, China

4. School of Basic Medical Sciences, Ningxia Medical University, Yinchuan, 750000, Ningxia, China

5. Department of Pathogenic Biology and Medical Immunology, Ningxia Key Lab of Common Infectious Disease, School of Basic Medical Sciences, Ningxia Medical University, Yinchuan, 750000, Ningxia, China

6. College of Traditional Chinese Medicine, Ningxia Medical University, Yinchuan, 750000, Ningxia, China

*Correspondence: Shaobin Jia, professor, Email: jsbxn@163.com;

Hao Wang, professor, Email: wanghaograduate@126.com;

Xiaoxia Zhang, professor, Email: zxx1216@163.com

# These authors contributed equally to this work.

Abstract

The gut microbiome shape the host immune system and influence the outcomes of various cardiovascular disorders, meanwhile, it is a malleable microbial community that can be remodeled in response to various factors, including medications. Experiment

implicated ticagrelor, one of the P2Y12 inhibitors, exerted antibacterial activity against gram-positive bacteria established from clinical evidence that it could reduce the incidence of infection-related disease. Here we performed 16S rRNA and metagenomic analysis from patients with unstable angina pectoris (UAP) treated with ticagrelor plus aspirin or clopidogrel plus aspirin for one month to determine the composition and functions of the gut microbiome difference between the two main medications. Our results suggested that the functional peptidoglycan (PGN) and *Staphylococcus aureus* (*S. aureus*) infection biosynthesis pathways were downregulated with ticagrelor-aspirin treatment in the gut. Furthermore, we found these changes were accompanied by increasing peripheral regulatory T cells (Tregs) and ectonucleotidases CD39/CD73 expressions with responding to ameliorating inflammation. To further validate the result, 16S rRNA and metabolomic analysis were carried out upon Western-diet (WD)-fed *ApoE*$^{-/-}$ mice, we found mice treated with ticagrelor plus aspirin exerted optimal synergistic effects on reducing the plaque burden and ameliorating inflammation through altered composition and functions of the gut microbiome which keeping in line with our clinical findings. The current study, for the first time, demonstrated the athero-protective effect of ticagrelor and displayed its therapeutic value at least partially attributed to its manipulation of gut microbiota.

Key Words: Atherosclerosis, gut microbiota, peptidoglycan, regulatory T cells, inflammation

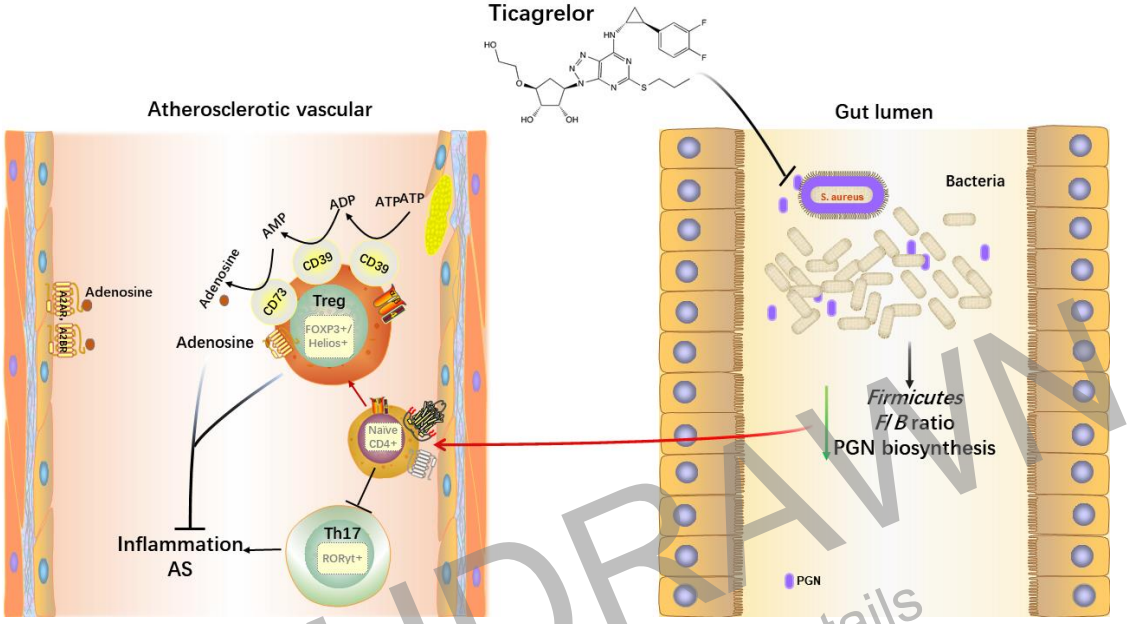

Graphic abstract

Ticagrelor acts on intestinal bacteria after oral administration, reducing several pathogenic Gram-positive (G^+) bacteria at phyla *Firmicutes* and the *Firmicutes*/*Bacteroidetes* (*F*/*B*) Ratio, thus decreasing the gut peptidoglycan (PGN) synthesis. The reduction of the above pathogenic factors causes the polarization of peripheral T lymphocytes toward Treg cells. The elevated Treg cells are accompanied by an increased expression of CD39/CD73 on Tregs, which hydrolyze the extracellular ATP generated from damaged endothelial cells into adenosine (ADO) with anti-inflammatory properties and ultimately inhibited the inflammation of atherosclerosis (AS).

Introduction

Based on numerous studies, atherosclerosis (AS) has now been considered chronic inflammation, various stimuli can trigger and sustain the inflammation. As one such stimulus, chronic infection shared the common pathophysiological milieu of chronic inflammation[1]. A distant or direct infection of vessel wall cells has been thought to be the cause or promoter of atherosclerotic plaques with the supports by finding the bacteria DNA in the plaques [2,3]. Actually, since the middle of the 1990s, bacterial or viral infections have been considered to involve in AS[4], it is increasingly believed that

gut flora, as comprises a treasure trove of immunomodulatory bacteria, has a cross-link to AS risk[5]. Numerous studies indicated that bacteria-derived metabolites like short-chain fatty acids (SCFAs)[6,7], bile acids (BAs)[8,9], and the high-profile Trimethylamine N-Oxide (TMAO)[10], regulated the risk of CVD. In addition to these metabolites, lipopolysaccharide (LPS) and peptidoglycan (PGN), known as the main components of the bacterial cell wall, can be recognized by the innate and adaptive immune system to reinforce the CVD pathogenesis potentially[5]. Unlike LPS restrict to gram-negative (G^-) bacteria, PGN is present in both G^- and gram-positive (G^+) bacteria, while is predominant in G^+ bacteria. A study enrolled 13 healthy individuals and 12 patients with symptomatic AS using metagenomes revealed that genes encoding PGN synthesis were enriched in patients' gut metagenomes [11]. In fact, two decades ago, PGN was found to gain access to atherosclerotic plaques and associated with the occurrence of a vulnerable plaque phenotype as a proinflammatory bacterial antigen[12]. Furthermore, a review recently highlighted the role of PGN as a determinative of brain inflammation[13]. All these facts indicated that gut PGN exerts a pro-inflammation profile in chronic inflammatory diseases, including AS. These collective findings have led to the idea that if the gut PGN biosynthesis pathway has been inhibited, can the atherosclerotic and related inflammation be ameliorated?

Adaptive immunity has a major impact on AS, with pro- and anti-atherosclerotic effects exerted by different subpopulations of T cells[14]. Regulatory T-cells (Tregs) are a subset of $CD4^+$ T cells with various immunosuppressive and anti-inflammatory functions[15]. The transcription factors Foxp3 and Helios are the master regulators of Tregs immunosuppressive functions[16,17]. It is well documented that the frequency of Tregs was reduced in the peripheral circulation of patients with carotid artery plaques[18]. Similarly, the number of Tregs was low in all stages of human atherosclerotic lesions, with measurements in surgical or biopsy samples[19]. It is well accepted that secretion of IL-10 by Tregs is important for the suppression, particularly in regulating inflammation against pathogens or foreign particles[20]. IL-10 has been found to play a role in prevention of AS and promotion of a stable plaque phenotype in *ApoE*$^{-/-}$ mice[21]. In

addition of IL-10, the mechanism of T cell on the suppression of inflammation should partially due to ectoenzymes CD39 (ENTPD1, ectonucleoside triphosphate diphosphohydrolase-1) and CD73 (NT5E, ecto-5′-nucleotidases) highly expressed on Tregs that can hydrolyze extracellular ATP generated from damaged vessel walls to adenosine (ADO), subsequently suppress effector T cells by binding to its receptor ADORA2A[22]. Another subset of $CD4^+$ T cells-T helpers 17 (Th17) mainly produce a strong pro-inflammatory cytokine IL-17A and have been observed in atherosclerotic plaques both in humans and animals[23,24]. The expression of transcription factor nuclear receptor RORγt characterizes the Th17 cells. It is controversial of the role of IL-17A in AS, with some study suggesting that IL-17A is pro-atherogenic or athero-protective [24,25], and a further study suggesting that IL-17A has no effect on AS[26].

Dual antiplatelet therapy (DAPT), consisting of aspirin and a P2Y12 inhibitor, ticagrelor or clopidogrel, is essential for the prevention and treatment of recurrent thrombotic events in patients with ACS or MI[27]. As a new P2Y12 inhibitor, ticagrelor can bind to its receptor P2Y12 reversibly to conduct effect without liver enzyme metabolism. Notably, a handful of clinical trials have established the superiority of ticagrelor against ACS, including the study that ticagrelor could significantly reduce the major adverse cardiovascular events (MACE) as compared to clopidogrel in patients with ACS[28] and provided ongoing benefits if continued long term[29]. Based on a current meta-analysis, ticagrelor could significantly reduce recurrent myocardial infarction[30]. Furthermore, a *post hoc* analysis indicated that ticagrelor could lower the mortality following pulmonary adverse events and sepsis compared to clopidogrel in the PLATelet inhibition and patient outcomes (PLATO) trial[31]. Evidence continued to mount that, ticagrelor exerted the potential of improving lung function in inpatients with pneumonia[32]. Taken together, these observations indicated the inevitable role of ticagrelor in reducing the incidence of infection-related disease while functioning its antiplatelet profile. Herein, scientists performed a study *in vivo* and *in vitro* that uncovered ticagrelor and its major metabolite AR-C124910 had antibacterial activity

against all G^+ strains tested and was inefficient against G^- strains even in a higher concentration[33].

Despite the studies above demonstrated the anti-bacteria signature of ticagrelor *in vivo* and *in vitro*, the impact of this first-line clinical medication on host gut microbiome has not been experimentally verified, where the constant dialog between gut microbiome and immune system take place. Herein, the driving concept of this study is to explore the athero-protective effect of ticagrelor in improving the immuno-inflammation via modifying the gut dysbiosis both in humans and experimental mice. Considering the privilege of its anti-bacterial characteristic, and the given close relationship of microbiota-immune interactions during the inflammation[34,35], we therefore hypothesized that ticagrelor may regulate the gut microbiota, in particular, reduce the synthesis of PGN in gut, thus potentiate anti-inflammatory property via regulating the immune system of Treg/Th17 axis. To explore the hypothesis, we attempted to comprehensively profile the composition and function of the gut microbiota by 16S rRNA sequencing and metagenomes in unstable angina pectoris (UAP) patients with the intervention of ticagrelor plus aspirin or clopidogrel plus aspirin as antiplatelet therapies, the inflammation and adaptive immunity related regulators Tregs, CD39/CD73 Tregs and Th17 cells have been detected simultaneously. To substantiate the hypothesis, mice experiment was conducted parallelly to exclude the interference factors in humans. Finally, the intervention with ticagrelor after depletion of the gut microbiome by antibiotics in mice was elicited to confirm whether the microbiota plays an indispensable role in immuno-inflammatory regulation by ticagrelor.

Results

Characteristics of the study population

From July 12 to December 25, 2021, a total of 103 participants of UAP patients were screened. 75 patients were enrolled, with 39 assigned to the ticagrelor-aspirin (TA) group and 36 allocated to the clopidogrel-aspirin (CA) group, in parallel with matched

ages, gender, and BMI. Finally, 11 patients in the TA group and 10 patients in the CA group donated their fecal and blood samples on admission and one-month follow-up in the study. The clinical characteristics and concomitant medications use of the 21 patients were summarized in **Table 1**. There was no significant difference of previous and medications history, nor of the laboratory variables. All subjects in two groups underwent percutaneous coronary intervention (PCI) for the treatment of vessel narrowing and occlusion.

TA decreased the PGN and *S. aureus* infection biosynthesis pathways. We performed a detailed comparison of gut microbial profiles using 16S rRNA gene sequencing and metabolomics in the fecal samples. The Shannon index at phylum level in TA group revealed a tendency toward alpha diversity compared with CA group (P=0.054, **Figure 1a**), in terms of β diversity, there was no distinct features between the two groups at the phylum level (**Figure 1b**). The relative abundance of phyla *Firmicutes* was visibly lower in the TA group than CA group (P=0.06, **Figure 1c**), but there were no differences in phyla *Bacteroidetes* or *Firmicutes* / *Bacteroidetes* (*F*/*B*) ratio (**Figure 1c**). Next, we used gut metagenomics to explore the functional pathways that the two different medications may influence. Surprisingly, we found the PGN biosynthesis pathway as the highest proportion of the whole functional pathways was lower in the TA group (the first red rectangle, **Figure 1d**). PGN biosynthesis contributed to *S. aureus* proliferation, which was also limited under TA treatment (The second red rectangle, **Figure 1d**). The KEGG map of PGN biosynthesis was generated and displayed associated with the *S. aureus* after two different treatments (**Figure 1e**). Strikingly, we found two PGN biosynthetic enzymes 3.4.6.14 and 1.3.1.98, especially the most predominant 3.4.6.14, were less enriched in the gut metagenomes under TA treatment (**Figure 1f**). The baseline of the two pathways and enzymes had no significant differences between the two groups (**Figures 2Sa-d**). Our data collectively suggested that ticagrelor played a potential role in regulating gut microbial dysbiosis in AS.

Alterations of gut microbiota in patients with TA correlated with increased Tregs. Plenty of clinical and animal experiments indicate that AS is an inflammatory disease which is involved in the onset and progression of the disease. Accumulating evidence solidly demonstrate that microbial dysbiosis notably affects the inflammatory statement in AS[36] and T cells play a pivotal role in cross-linking of the inflammation and dysbiosis of intestinal flora in AS [34]. Therefore, we hypothesized that the alteration of gut microbiota in AS patients with the two different antiplatelet therapy at least partially affected the adaptive immune system through regulating Treg/Th17 balance and subsequent inflammation indicators in peripheral circulation. We assessed the mentioned immune cells by flow cytometry and observed an increased frequency of $Foxp3^+$ Tregs and $Foxp3^+Helios^+$ Tregs in the PBMC after one-month TA treatment (**Figure 2a, b, e, f**). $Helios^+$ Tregs was increased in TA group compared to the baseline, while in the CA group there was nearly significant difference from baseline (P=0.07) or TA group (P=0.06) (**Figure 2c, d**). There was also a significant reduction of $IL17A^+CD4^+$ T helper cells in TA group and a visible reduction in the CA group from the baseline (P=0.054), nevertheless, there was no significant difference between two treated groups (**Figure 2g, h**). As the nuclear transcription factor of Th17, the expression of RORγt was measured, but no difference was found between pre or after treatment for each medication compared to baseline, as well as between TA and CA (**Figure 2i, j**). Meanwhile, qPCR was used to investigate the mRNA levels of *Foxp3*, *Helios*, *RORC*, together with the inflammation cytokines *IL-17A*, *IL-10*, *TNF-α* in PBMC, the results indicated that neither treatment significantly modified the *Helios* or *RORC* expression from baseline or between treated groups (**Figure S4a, b**). The expression of *Foxp3* was elevated in TA group from baseline but not differed from CA group (**Figure S4c**). The mRNA levels of *IL-17A*, *IL-10*, *TNF-α* were consistently decreased in two treated groups from baseline, but there was no significant difference between the treated groups except *TNF-α*. (**Figure S4d, e, f**). Finally, the plasma levels of IL-10 and IL-17A were detected by ELISA. Unfortunately, the concentration of IL-10 was not affected in two treatments from baseline nor between TA and CA (**Figure**

S4g). Either use of TA or CA could decrease the IL-17A level, but there still showed no significant difference between the parallel treatments (**Figure S4h**). These findings indicated that TA exerted the anti-inflammatory profile by up-regulating Tregs, but irrelevant to the Th17 cells and the production of IL-10 or IL-17A.

CD39-CD73-adenosine signaling is essential for TA mediated anti-inflammation. CD39-CD73 expressed on Tregs played a component role in immunosuppression, that can hydrolyze the extracellular ATP (eATP) released by dying or damaged cells into ADO[37], and it functions as anti-inflammation in many impaired vessels including the atherosclerotic vessels. As illustrated in our previous findings, we next tried to detect the expression of CD39-CD73 on Tregs by flow cytometry. Our results revealed that $CD39^+$ Tregs could be elevated both in the TA and CA groups, while TA exerted better effect than CA (**Figure 3a, b**). A significant elevation of $CD73^+$ Tregs was observed in TA but not in CA from the baseline, but no superiority was seen between TA and CA (P=0.06) (**Figure 3c, d**). Because of fast degradation of ADO within seconds, we tested the mRNA levels of ADO receptors including *ADORA2A*, *ADORA2B* in PBMC. The outcome showed that *ADORA2A* and *ADORA2B* gene expression could be increased in TA compared to pretreatment. In contrast, we didn't see any significant changes of *ADORA2A* and *ADORA2B* gene expression in CA treatment compared to the baseline. When it came to compare the two genes between CA and TA, we could visibly see a higher expression in TA group but without statistically significance, the P values were 0.051 and 0.08 respectively (**Figure 3e, f**). These observations implied that CD39 and CD73 expressed on Tregs could influence peripheral inflammation, further emphasizing the therapeutic potential of ticagrelor targeting these molecules in AS.

TA might exert optimal synergistic effects on anti-atherosclerosis profile in *ApoE*$^{-/-}$ mice. To investigate the effects of different antiplatelet medicine alone or combinations, which mimic the clinical applications, *ApoE*$^{-/-}$ mice were treated by Ticagrelor (Tica), Ticagrelor+Aspirin (TA), Clopidogrel (Clop), Clopidogrel+Aspirin

(CA), Aspirin (Asp) and vehicle as control (Model) respectively. As the basic indicators, body weight, total bile acid, and lipid profiles exerted no statistical differences among the diverse groups (**Figure S4a-g**). Oil Red O staining of the atherosclerotic areas both in whole aorta and aorta sinus presented that compared to model, atherosclerotic lesion formation was markedly decreased in Tica and TA treated. Notably, TA exhibited better plaque burden attenuation than the other groups (**Figure 4b-e**, **h**). Any single use of Tica, Clop, Asp or combinations TA and CA could elevate the collagen deposition (**Figure 4f, h**), suggesting that the medications promoted the stability of atherosclerotic plaques. Collectively, these pathological detections indicated that *ApoE*$^{-/-}$ mice received either Tica, Clop, Asp alone or combination TA, CA, they all could ameliorate atherosclerostic plaques, of particular, TA seemed to exert optimal syneristc effects on athero-protective property.

TA modulated the gut dysbiosis in *ApoE*$^{-/-}$ mice to meet an analogous character presented in human, confirmed its mechanism of TA in decreasing the gut PGN biosynthesis and *S. aureus* infection pathways. PCR-free library was constructed based on Illumina Nova sequencing platform sequencing, and then Paired-End sequencing was performed. By splicing Reads, an average of 97,264 tags were measured per sample, and an average of 90,830 valid data were obtained after quality control. The rarefaction curves of all the samples displayed the sequence number nearly to 50000, indicating the sequencing depth was adequate (**Figure S5a**). In terms of alpha diversity, we observed significant differences between TA vs Model (P<0.05), TA vs Asp (P<0.05), and TA vs CA (P<0.05) (**Figure 5a**) by Shannon's index. To further evaluate the overall gut microbiota community, β diversity of PCA based on the weighted UniFrac distances was conducted (**Figure 5b**), single Tica or Clop exhibited different compared to Model (P<0.01) and Asp (P<0.01), while the combination TA showed no significant differences from other groups. According to the species annotation results, the maximum value sorting method was used to select the top 5

species with the largest abundance in each group with generating a Sankey diagram. The Sankey diagram can intuitively view the relative abundance and distribution at the phylum level (**Figure 5c**). We could obviously conclude that in Tica and TA groups, the most predominant taxa were *Bacteroidota* and *Verrucomicrobiota*, the proportion of *Firmicutes* came to the third place of the whole phylum level (**Figure 5c**). Clop could really upregulate the *Firmicutes* population, while CA or Asp showed no obvious changes compared to Model by visual inspection (**Figure 5c**). To further explore the relative proportion of dominant taxa at the phylum and genus levels, we conducted Matastat analyze in groups (**Figure 5d, e**). As expected, *Firmicutes* were reduced remarkably in Tica and TA group compared to other groups (**Figure 5d**), which was consistent with our previous clinical findings (**Figure 1b**). Notably, the phyla *Desulfobacterota* in CA treated group exhibited higher proportion compared to Model or to other treatments ($P<0.01$, **Figure 5d**), which was reported as opportunistic pathogens in obese mice[38]. The *F*/*B* ratio decreased dramatically in Tica and TA compared to model and Clop related treatments, while Clop and CA changed the *F*/*B* ratio very slightly and had no significant difference compared to Model (**Figure 5f**). It is reported that *Firmicutes* and *F*/*B* ratio were positively related to AS progression[39]. At genus level, we noted that, Tica and TA could sharply reduce the *Bilophila*, *Blautia, Clostridium_sensu_stricto_1,* and *[Eubacterium]_fissicatena_group* compared to Model, Clop or CA treatments (**Figure 5e**), all these species were catalog of phylum *Firmicutes* (**Figure S5d**) and were considered pathogenic bacteria except *Blautia*. Instead, *Parasutterella*, *Muribaculum* were significantly elevated in TA, while *Faecalibaculum* and *Roseburia* both of them are phyla *Firmicutes*, were incredibly increased in Tica group (**Figure S6f, g**). In addition, the genera *Akkermasia* contributed to phyla *Verrucomicrobiota* increase in Tica group (**Figure 5e, S5e**). Finally, the functional pathways were predicted by Tax4fun. Encouragingly, the gut PGN biosynthesis and *S. aureus* infection pathways were obviously limited by TA treatment (**Figure 5g, h**), which confirmed our previous findings in human study.

Treg/Th17 axis and CD39-CD73 signaling are essential for Tica and TA-mediate anti-inflammation effect in *ApoE*$^{-/-}$ mice. In view of the effectiveness of Tica and TA on atherosclerotic plaque burden amelioration and the gut microbiota regulation in mice mentioned above, we further investigated the Treg/Th17 axis, due to abundant studies indicated that PGN and *S. aureus* had close relationship with T cell differentiation and the inflammation[13,40-42]. Hence, we investigated the Treg/Th17 cells proportions in blood and inflammation indicators in plasma. Single Foxp3^{+}Treg, or Helios^{+}Treg, as well as both Foxp3^{+} Helios^{+}Treg cells were obviously elevated in Tica and TA compared to model and other treatments, while we didn't see such effects in Clop and CA treatments (**Figure 6a-f**). Unlike our human study, in mice model the Th17 cells were remarkably reduced in all treated groups compared to Model, meanwhile TA exhibited most conspicuous effect (**Figure 6g, h**). To assess the inflammatory indicators in diverse groups, Cytometric Beads Array (CBA) was used to detect the pro-inflammatory IFN-γ, IL-1β, IL-6, MCP-1, TNF-α, IL-17A and anti-inflammatory IL-10. Both P2Y12 inhibitors had a marked effect on inflammatory indicators response by reducing pro-inflammatory cytokines compared to Model, and there was no significant difference between them (**Figure 6i**). TA showed distinct feature in lowering the IL-17A level, while in increasing IL-10, Tica did better compared to Model and other groups (**Figure 6i**). To clarify the relationship of CD39, CD73 and ADO, we detected the co-expressions of CD39, CD73 and ADO receptors with immunofluorescence staining in aorta sinus. Both the areas of CD39^{+}ADORA2A^{+} and CD73^{+}ADORA2A^{+} were increased in all treatments, while Tica and TA exhibited excellent effects than other medicine (**Figure 7a-d**). We previously mentioned that eATP can damage vessel wall, which can be conversed to ADO by CD39 and CD73 step by step. Hence, we tested the plasma ATP concentration to confirm whether higher expression of CD39 and CD73 correlated with lower ATP. Notably, in Tica and TA groups, the concentration of ATP could be reduced obviously compared to other groups (**Figure 7e**). Surprisingly, CA reduced the ATP concentration as well, the explanation maybe, besides CD73 and CD39, ADO can also be generated by alkaline through phosphatases sequential removal

of phosphate groups from ATP[43]. Correlation analysis indicated that both elevated expressions of $CD39^+ADORA2A^+$ and $CD73^+ADORA2A^+$ had a negative correlation with plasma ATP concentration (**Figure 7f, g**), thus revealing that the anti-inflammatory ADO may generate from the hydrolysis of ATP by CD39 and CD73.

Microbiome depletion terminated the athero-protective profile by ticagrelor. To explore the association between the gut microbiome and athero-protective profile by ticagrelor in *ApoE*$^{-/-}$ mice, we treated 8-week-old mice with an antibiotic cocktail (ABX) for 5 weeks to establish an antibiotic-induced microbiome depletion condition. Depletion of microbiota with ABX was confirmed by qPCR using universal 16S rRNA primers. After 5 weeks of ABX, mice were treated with ticagrelor (TABX) or vehicle (MABX) as control respectively. The plaque burden of the whole aorta and aorta sinus in TABX did not differ from those of control mice (**Figure 8b-e**). Consistent with the atherosclerotic plaques, significant difference of the frequencies of $Foxp3^+Helios^+$ Tregs, $IL17A^+CD4^+$ T helper cells and inflammatory cytokines were not observed in ABX induced mice in absence of ticagrelor or not (**Figure 8f-j**). These findings strengthened our hypothesis that ticagrelor exerted as an immuno-inflammatory modulator in the context of AS in a microbiome-dependent manner.

Discussion

The immune system is a complex network composed of innate and adaptive components with an excellent capacity to adapt and respond to highly diverse challenges. Collectively, this network acts as a rigid regulator of host homeostasis in the context of microbial and environmental encounters. Studies have uncovered the critical role of the microbiota in promoting and balancing all aspects of the immune system[44,45]. Growing evidence indicate that microbial alterations have been shown to regulate the inflammatory response and adaptive immune system, which is required for host defense against intestinal infections[46-48]. Among the adaptive immune system,

Tregs and Th17 cells play a pivotal role in sustaining and restoring homeostasis in diseases[49,50], including cardiovascular disease[51].

In this work, we have shown both clinical and murine measures to explore the gut microbiome changes regulated by the first-line clinical platelet-modifying medicine, the P2Y12 inhibitors, ticagrelor and clopidogrel. Our results suggested that ticagrelor or ticagrelor combined aspirin function as bacterial growth modulators in the gut and exerted their effectiveness in reducing the phylum *Firmicutes* and *F/B* ratio, which was considered to be harmful to atherosclerosis[39], thus decreasing the gut PGN and *S. aureus* infection biosynthesis to prevent the development of AS. Our data indicated that the observed reduction of gut PGN biosynthesis resulted from altered enzymes that contributed to the pathway of PGN biosynthesis by the remodeled gut microbiota, which subsequently, led to the downregulation of *S. aureus* infection biosynthesis. In addition, ticagrelor and ticagrelor-aspirin in regulating gut flora suppressed the production of pro-inflammatory cytokines, increased the relative population of the circulatory of Tregs, including $Foxp3^{+}$Treg, $Helios^{+}$Treg, $Foxp3^{+}Helios^{+}$Treg immune cells, and the elevated production of CD39/CD73 expressed on Treg cells which can hydrolyze the extracellular ATP (eATP) generated from damaged endothelial cell to ADO contributed to the anti-inflammatory effect as well. However, there was no statistical difference in Th17 cells under the two different treatments, which is in line with the findings of the controversial role of Th17 in AS[9,24,52,53]

Indeed, since the *post hoc* analysis of the PLATO trial indicated that ticagrelor was superior to clopidogrel in infectious-related diseases, studies focused on ticagrelor in reducing the *S. aureus* infection were popped out[54-57]. Our findings for the first time provided evidence for gut microbiome-dependent anti-inflammation properties of ticagrelor, which indicated that ticagrelor could affect the immuno-inflammation system in addition to its well-known antiplatelet effects. Phyla *Firmicutes* and *Bacteroides* are the most predominant taxa in the human and murine gut, and it is widely accepted that decrease of *Bacteroides*, increase of *Firmicutes* and the ratio of *Firmicute* to *Bacteroides* (F/B) contributed to promoting atherosclerosis[39]. Most of the

G^+ bacteria contribute to the *Firmicutes*. Surprisingly, we found *Firmicutes* were decreased after ticagrelor-aspirin intervention compared to clopidogrel-aspirin. In the mice study, we found the genera *Bilophyla*, *Clostridium_sensu_stricto_1* and [*Eubacterium*]*_fissicatena_group* reduced remarkably after the treatment of ticagrelor or ticagrelor-aspirin, these species generated from Phyla *Firmicutes*, were considered pathogen-related bacteria as well[58-61]. *Blautia*, derived from phyla *Firmicutes*, with potential probiotic property[62], was sharply reduced with the treatment of ticagrelor or ticagrelor-aspirin, while enriched in clopidogrel-aspirin or aspirin. These intricate results led us to determine the production of SCFAs, for one of the SCFAs, the butyric acid generated from most of the phyla *Firmicutes*. Surprisingly, all of the SCFAs increased slightly in ticagrelor, or ticagrelor-aspirin treated groups (**Data available**), together with the genera *Faecalibaculum* and *Roseburia* contributed to phyla *Firmicutes* incredibly enriched in ticagrelor treated group, these data reinforced the concept that ticagrelor functions as modifying the microbiome even though it targets the phylum *Firmicutes*. Meanwhile, the metagenome analysis uncovered that the bacterial PGN biosynthesis was limited by ticagrelor. PGN, a well-known component of the bacterial cell wall, is especially prominent in G^+ bacteria (up to 70 layers), can exert robust inflammatory effects[63], including T cell polarizing cytokines, which are required for T helper cells activation[64]. In our study, we found a decreased biosynthesis of PGN under ticagrelor-aspirin treated accompanied with increased production of peripheric Tregs, while mice were under antibiotic-induced microbiome depletion, the proportion of Tregs kept at the same level in presence or absence of ticagrelor, which validated the hypothesis of microbiota-mediated anti-inflammation and immune regulation by ticagrelor.

Tregs mediated suppression functions as negative regulation of immune-mediated inflammation and features prominently in acute and chronic infections, cancer, and metabolic inflammation[65]. *Foxp3*, the transcription factor that specifies the Treg cell lineage, essential for Treg cell differentiation and suppressor function and defines the Treg cell lineage[65,66]. *Helios* (*IKZF2*) belongs to the *Ikaros* transcription factor family,

is found critically required to maintain a stable Treg cell phenotype in the inflammatory diseases in recent years[67]. To be noted, studies indicated *Helios* enhances regulatory T cell function in cooperation with *Foxp3* in patients with rheumatoid arthritis[68]. Our results demonstrated that the treatment with ticagrelor could obviously up-regulate the expression of $Foxp3^+$ Tregs, $Helios^+$ Tregs, and $Foxp3^+Helios^+$ Tregs, which displayed suppressor function of adaptive immune system in AS. By contrast, a previous study which enrolled volunteers to determine the two main P2Y12 inhibitors response to systemic inflammation by injection of *Escherichia coli* endotoxin, the result of the study indicated that ticagrelor could obviously increase the anti-inflammatory cytokine IL-10, however, we didn't see any perturbation of IL-10 level under established groups. Discrepancies between our findings and this previous report may be explained as a cytokine related to Tregs, IL-10 is produced by other type of cells as well, such as macrophage, mast cell, eosinophils, neutrophils, B cells, natural killer cells and dendritic cells, resulting the dual function of anti- and pro-inflammation[69]. Additional explanation of stable level of IL-10 after using the P2Y12 inhibitors may on account of little is known about the interplay of IL-10 and other pro-/anti-inflammatory cytokines in the pathogenesis of AS. In recent years, Th17 cells, a subset of $CD4^+$ T cells, were found to be pro- and anti-atherogenic effects[70]. In our study, single use of P2Y12 inhibitors or they combined with aspirin respectively could reduce the production IL-17A compared to baseline, which in line with the study that ticagrelor and clopidogrel could obviously reduce the development of Th17 cells in EAE, an experimental multiple sclerosis model[71]. But we found there was no superiority of ticagrelor to clopidogrel. IL-17A is the cytokine that produced by Th17 cells, but γδ T cells represent another source of IL-17 in intestinal. Our unshown data of mice exhibited no difference population of γδ T cells in the diverse groups. Furthermore, IL-17 family members contain IL-17A, IL-17B, IL-17C. IL-17D, IL-17E, IL-17F, the crosslink of these IL-17 family members in AS has not yet been studied. It seemed like that in our study, Tregs and Th17, partners of trading off and taking turns, left elevated Tregs to display the suppressor function generated by ticagrelor via a microbiota-dependent manner.

eATP as a kind of danger-associated molecular patterns (DAMPs), binds to purinergic receptors to trigger signaling cascades to induce an inflammatory response[72]. A mice model clarified the fact eATP increased released in AS and enhanced AS via binding to its receptor P2Y2 through leukocyte and monocyte recruitment[73]. CD39, together with CD73, both ectoenzymes that hydrolyze eATP to pericellular ADO step by step. Evidence elucidated the absence of CD39 and CD73 exacerbate the progression of AS[37,74]. Extracellular ADO exerts its biological effects through the engagement of 4 distinct subtypes of ADO receptors, namely, ADORA1, ADORA2A, ADORA2B and ADORA3 receptors. Immunosuppressive activities of ADO are mainly mediated by Gs-coupled ADORA2A and ADORA2B receptors[75]. Researchers concluded that CD39 and CD73 are surface markers of Tregs that impart a specific biochemical signature characterized by ADO generation that has functional relevance for cellular immunoregulation[22]. In the current study, we detected the ADO receptors, ADORA2A and ADORA2B as indirect markers of ADO due to the fast degradation of ADO within seconds by no effective means. Our data suggested that altered microbiota induced by ticagrelor or ticagrelor-aspirin activated the Tregs and their increased production of CD39 and CD73 might limit the systemic inflammation in AS.

In conclusion, ticagrelor or ticagrelor-aspirin mediated multiple alterations of composition and function in gut microbiota, ameliorated inflammation status, and uncovered a potential mechanism of CD39-CD73-Treg associated with better AS outcomes beyond the function as P2Y12 inhibitors. Our findings shed new light on the implication of the intestinal microbiota–immune system–cardiovascular axis in atherosclerotic development by the intervention of ticagrelor or tiagrelor-aspirin, specifying the indication of ticagrelor in infection related disease via modifying the gut microbiota.

Materials and Methods

Study population

A total of 103 patients with UAP were screened in, 11 of whom took Ticagrelor+Aspirin (TA) and 10 with Clopidogrel+Aspirin (CA). All patients should meet the inclusion criteria as follows: 1. Coronary atherosclerotic plaques confirmed by coronary computed tomography angiography (CCTA) or coronary angiography (CAG); 2. Age between 40-70 years old; 3. No previous history of antiplatelet therapy. Patients with: 1. Infectious, genetic, autoimmunity-mediated, metabolic diseases; 2. Digestive disorders (inflammatory bowel disease, acute/chronic diarrhea, chronic constipation); 3. Severe hepatic and renal insufficiency; 4. Chronic respiratory diseases (COPD, asthma, etc.); 5. Antibiotics treatment within the past 1 month with the course of treatment exceeding 3 days were excluded. The enrollment strategy was displayed in **Figure S1**. Peripheral venous blood and fecal samples were collected on admission and one-month follow-up for every enrolled patient. Plasma and PBMCs were isolated from each fresh blood sample, and PBMCs were prepared for the subsequent experiments of flow cytometry and mRNA extraction. The stool samples were collected and immediately stored at -80°C for further study. The study was conducted in accordance with the declaration of Helsinki. All subjects provided written, informed consents for the participation of the study. All blood and fecal samples were collected with ethics approval from the General Hospital of Ningxia Medical University (No. KYLL-2021-432). The study was registered at Chinese Clinical Trial Registry (Registration number ChiCTR2100051564).

Animals and Experimental design

Seventy-two male *ApoE*$^{-/-}$ mice (C57BL/6J) and 10 male C57BL/6J mice were purchased at 5 weeks of age and were housed in under SFP conditions at 22°C with a 12h light/dark cycle and free access to water and food. Up to 5 mice were allocated per cage and had three weeks of adaptation time with a chow diet before the experiment. Mice were fed with a Western diet containing 0.5% cholesterol together with different treatments of administration of Tica (Ticagrelor; Brilinta, 120mg/kg/day), Clop (Clopidogrel; Plavix, 48mg/kg/day), Asp (Aspirin; Bayer S.p.A, 67mg/kg/day) and the combination of TA (ticagrelor 120mg/kg/day+Aspirin 67mg/kg/day), CA (Clopidogrel

48mg/kg/day+Aspirin 67mg/kg/day) and vehicle as control (Model) respectively for 15 weeks. Dosage of ticagrelor was known to provide comparable platelet inhibitory effect in mice[76], and dosages of clopidogrel and aspirin were 0.42 and 0.56-fold to ticagrelor corresponding to the dosages used in humans[77]. For antibiotic-induced microbiome depletion, the mice were supplied antibiotics cocktail (ABX, consisting of ampicillin 1 g/L, vancomycin 500 mg/L, neomycin 1 g/L, and metronidazole 1 g/L, all of them were bought from Sigma) to deplete gut commensal bacteria in their drinking water for 5 weeks, and fresh ABX was replaced every other day. At the end of the study, animals were euthanized with 4% sodium pentobarbital and sacrificed for the subsequent study. This animal experiment has been approved by Laboratory Animal Ethical and Welfare Committee of Ningxia Medical University (No. 2020-078).

16S rRNA sequencing, processing, and analyzing of the gut microbiota

Total microbial genomic DNA was extracted from fecal samples of humans and mice using the E.Z.N.A.® DNA Kit (Omega Bio-Tek, Norcross, GA, U.S.) according to the manufacturer's instructions. The quality and concentration of DNA were determined by 1.0% agarose gel electrophoresis and a Nano Drop® ND-2000 spectrophotometer (Thermo Scientific Inc., USA) and kept at -80 ℃ prior to further use. The hypervariable region V3-V4 of the bacterial 16S rRNA gene was amplified with primer pairs 338F (5'-ACTCCTACGGGAGGCAGCAG-3') and 806R (5'-GGACTACHVGGGTWTCTAAT-3') by an ABI Gene Amp® 9700 PCR thermocycler (ABI, CA, USA). The PCR reaction mixture included 4 μL 5× Fast Pfu buffer, 2 μL 2.5 mM dNTPs, 0.8 μL each primer (5 μM), 0.4 μL Fast Pfu polymerase, 10 ng of template DNA, and ddH_2O to a final volume of 20 μL. All samples were amplified in triplicate. The PCR product was extracted from 2% agarose gel and purified using the AxyPrep DNA Gel Extraction Kit (Axygen Biosciences, Union City, CA, USA) according to manufacturer's instructions and quantified by Quantus™ Fluorometer (Promega, USA). Purified amplicons were pooled in equimolar amounts and paired-end sequenced on an Illumina MiSeq PE300 platform (Illumina, San Diego, USA) according to the standard protocols. After demultiplexing, the resulting sequences were filtered with fastp for

quality control (0.19.6)[78] and merged with FLASH (v1.2.11)[79]. Then the high-quality sequences were denoised using DADA2[80] plugin in the Qiime2[81](version 2020.2) pipeline with recommended parameters, which obtained single-nucleotide resolution based on error profiles within samples. DADA2 denoised sequences are usually called amplicon sequence variants (ASVs). To minimize the effects of sequencing depth on alpha and beta diversity measurement, the number of sequences from each sample was rarefied to more than 40,000, which still yielded an average good's coverage of 97.90%. Taxonomic assignment of ASVs was performed using the Naive Bayes consensus taxonomy classifier implemented in Qiime2 and the SILVA 16S rRNA database (v138). The metagenomic function was predicted by Tax4Fun [82] in mice experiment.

Bioinformatic analysis of the gut microbiota was carried out using the Majorbio Cloud platform (https://cloud.majorbio.com). Based on the ASVs information, rarefaction curves and alpha diversity indices including observed ASVs, Shannon index was calculated with Mothur v1.30.1. The similarity among the microbial communities in different samples was determined by PCA (Principal Component Analysis) based on Bray-curtis dissimilarity using Vegan v2.5-3 package in human data or by weighted unifrac in mice. The MetaStat analyzing was used to perform with the hypothesis testing on the species abundance data between groups in different levels and q-values were obtained by the correcting p-values to assess the significant differences between groups. *P* values of <0.05 were considered statistically significant.

Metagenomic analysis

Total genomic DNA was extracted from human fecal samples using the E.Z.N.A.® DNA Kit (Omega Bio-tek, Norcross, GA, U.S.) as manufacturer's instructions. Concentration and purity of extracted DNA were determined with TBS-380 and NanoDrop2000, respectively. DNA extract quality was checked on 1% agarose gel. DNA extract was fragmented to an average size of about 400 bp using Covaris M220 (Gene Company Limited) for paired-end library construction, which was constructed using NEXTFLEX® Rapid DNA-Seq (Bioo Scientific, Austin, TX, USA). Paired-end sequencing was performed on Illumina NovaSeq (Illumina Inc., San Diego, CA, USA)

563 at Majorbio Bio-Pharm Technology Co., Ltd. using NovaSeq reagent kits according to
564 the manufacturer's instructions (www.illumina.com).

565 The data were analyzed on the free online platform of Majorbio Cloud Platform
566 (www.majorbio.com). Briefly, the paired-end Illumina reads were trimmed of adaptors,
567 and length<50 bp or with a quality value <20 or having N bases were considered low-
568 quality reads and were removed by fastp[78] (https://github.com/OpenGene/fastp, version
569 0.20.0). Reads were aligned to the human genome by BWA[83] (http://bio-
570 bwa.sourceforge.net, version 0.7.9a) and any hit associated with the reads and their
571 mated reads were removed. Metagenomics data were assembled using
572 MEGAHIT[84](https://github.com/voutcn/megahit, version 1.1.2), which makes use of
573 succinct de Bruijn graphs. Contigs with a length ≥ 300 bp were selected as the final
574 assembling results used for further annotation. The KEGG annotation was conducted
575 using Diamond[85] (http://www.diamondsearch.org/index.php, version 0.8.35) and
576 transformed to the Kyoto Encyclopedia of Genes and Genomes database
577 (http://www.genome.jp/keeg/) with an e-value cutoff of $1e^{-5}$. Reads number relative was
578 used to downstream analysis. Two-side Wilcoson rank sum test was used to determine
579 gene abundance significant difference between groups. *P* values of <0.05 were
580 considered statistically significant.

581 **PBMC isolated from venous blood**

582 Peripheral blood mononuclear cells (PBMCs) were isolated from both human and mice.
583 After 5 ml of whole blood with EDTA-coated tube were collected and centrifugated at
584 600×*g* for 10 min, plasma was isolated and stored at -80℃ for further use. Then the
585 PBS was added to the rest of the blood and gently mixed. Next, the mixture was softly
586 underlayed on the Lymphocyte Separation Medium and centrifugated at 600×*g* for 25
587 min at room temperature. The ratio of blood, PBS, and Lymphocyte Separation Medium
588 was 1:1:1. PBMCs were harvested from the buffy coat layer and resuspended in media
589 contained 10% DMSO and 90% fetal bovine serum (FBS) and stored in liquid nitrogen
590 for downstream experiments.

591 **Quantitative determination of mRNA expression**

Total RNA were extracted from the fresh isolated PBMC, protocol was mention above, and E.Z.N.A.® Blood RNA Kit (OMEGA, #R6834) was used according to the manufacturer's instructions. cDNA was synthesized to a total of 500ng RNA in a 20 μL system using PrimeScript™ RT Reagent kit (TAKARA, #RR036A). q-PCR were performed on anlytik jena (qTOWER 2.0) PCR machine using Perfect Start Green qPCR Super Mix (TransGen, #AQ601). The program was performed as follows: 94℃ for 30 s, 94℃ for 5 s and 60℃ for 15 s, repeated for 40 cycles; 72℃ for 15 s (melt curve). Gene expression was analyzed using SYBR Green Master mix and selected primers used in this study were listed in **Table S1**. The expression of target genes was normalized to the expression of *β-ACTIN*, and shown as fold change relative to the pre-treatment group based on the $2^{-\triangle\triangle Ct}$ method.

Flow cytometric analysis (FACS)

PBMCs were quickly thawed at 37℃ and cell suspensions were adjusted to a density of 1×10^6 cells in 100 μL of medium (RPMI 1640 with 10% FBS) and stimulated with Cell Stimulation Cocktail (plus protein transport inhibitors) (500×) (eBioscience™, #00-4975) for 4 h at 37°C for Th17 staining whilst Foxp3/Transcription Factor Staining Buffer Set (eBioscience, #00-5523) was used for transcription factor staining as manufacturer's instructions. Cells were stained with antibodies listed below for surface and intracellular markers (4℃, 30 min). CD4-APC-eFluor 780 (eBioscience™, #47-0048), CD39-PE-Cy7 (eBioscience™, #25-0399), CD73-FITC (eBioscience, #11-0739), Foxp3-PE (eBioscience™, #12-4776), Helios-eFluor 450 (eBioscience™, #48-9983), RORγt-APC (eBioscience™, #17-6988), IL-17A-PE (eBioscience™, #25-7179), all these above were used for human study. In mice experiment, we used the antibodies as follow: CD4-FITC (eBioscience™, #11-0042), Foxp3-PE (eBioscience™, #12-5773), Helios-APC (eBioscience™, #17-9883), IL-17A-PC5.5 (eBioscience™, #11-7177). The fluorescent staining was performed after blocking the Fc receptor with the anti-CD16/CD32 antibody. FACS acquisition was performed with the cytometer Cytomics FC500 (Beckman Coulter). Finally, the Tregs and Th17 cells were analyzed by Beckman Cyto FLEX flow cytometer (Beckman Bioscience, United States).

621 **Measurement of cytokines in plasma**

622 LEGENDplex^{TM} Mouse Inflammation Standard Cocktail (Biolegend, #740371) was
623 used to measure the cytokines in plasma of the mice according to the manufacturer's
624 instruction. Samples were diluted as 1:2, a total of 7 standards were used per cytokine
625 to generate standard curve. Data were analyzed by LEGENDplex (version 8.0). For
626 human IL-10 and IL-17A cytokines' measurement, we used commercially available
627 ELISA kit, IL-10 (Boster, #EK0416) and IL-17A (Boster, #EK0430) following the
628 manufacturer's instructions.

629 **Histological analysis and immunofluorescence staining**

630 Frozen aortic roots were cut in 5 μm-thick serial cryosections and stained with Oil-Red
631 O, hematoxylin and eosin and Masson's trichrome respectively for the quantification of
632 lesion size and collage area. The whole aorta was isolated from carotid artery to iliac
633 artery and was stained with Oil-Red O to access the lesion area in general.
634 Atherosclerotic lesion of the whole aorta or aorta sinus staining above was observed
635 using the microscope (Olympus, Japan). For immunofluorescence staining, 5 μm-thick
636 sections of the frozen aortic roots were used to examine the expression of detected
637 antibodies. Briefly, sections were covered 10% goat serum to block the nonspecific
638 antigens at room temperature for 30 min. Then the sections were incubated with the
639 primary antibodies of anti-rabbit CD39, anti-rabbit CD73, anti-mouse ADORA2A
640 FITC (1:100, Santa Cruz, United States) overnight at 4°C. The next day, the slides were
641 incubated with a suitable secondary antibody conjugated goat anti-rabbit IgG-HRP for
642 1 h at room temperature. Finally, cell nuclei were mounted with DAPI for 10 minutes
643 at room temperature. Images were captured with blinded manner of Leica DMI3000+
644 DFC310FX fluorescence microscope (Leica, Germany). The positive areas in plaque
645 were quantified by Image-Pro Plus 6.0.

646

647 **Statistics**

648 Graphpad Prism (Version 8) and SPSS 22.0 were used for all the data analysis and the
649 value were expressed as the mean±SEM. The significant differences between groups

were calculated by unpaired Student's t test, or one-way ANOVA (Tukey's multiple comparison test). Normality and lognormality tests were carried out before the parametric analysis of Student's t test and one-way ANOVA. Welch's corrections were used when variances between the groups were unequal. Pearson correlation coefficient assay was used to analyze the expression correlation. Both significant differences ($P < 0.05$) and trends ($P < 0.1$) were reported where appropriate for all tests performed.

Abbreviations

AS: atherosclerosis; CVD: cardiovascular Disease; ACS: acute coronary syndrome; ASVD: atherosclerotic vascular disease; MI: myocardial infarction; UAP: unstable angina pectoris; MACE: major adverse cardiovascular events; AE: Adverse event; CCTA: coronary computed tomography angiography; CAG: coronary angiography; PCI: percutaneous coronary intervention; DAPT: dual antiplatelet therapy; TMAO: trimethylamine N-Oxide;; SCFA: short-chain fatty acid; LPS: lipopolysaccharide; PGN: peptidoglycan; 16S rRNA: 16S ribosomal RNA; Treg: regulatory T cell; eATP: extracellular ATP; ADP: adenosine diphosphate; AMP: adenosine monophosphate; ADO: adenosine; ADORA2A: adenosine receptor A2A; ADORA2B: adenosine receptor A2B; KEGG: Kyoto Encyclopedia of Genes and Genomes;

Competing Interests

The authors have declared that no competing interest exists.

Data availability

Sequence data of 16S rRNA and metagenome that support the findings of this study have been deposited in National Center for Biotechnology Information (NCBI) with the primary accession code: SRP371254. Raw data of SCFA will be made available from the corresponding author upon reasonable request.

References

1 Li, B., Xia, Y. & Hu, B. Infection and atherosclerosis: TLR-dependent pathways. *Cell Mol Life Sci* **77**, 2751-2769, doi:10.1007/s00018-020-03453-7 (2020).

2 Ott, S. J. *et al.* Detection of diverse bacterial signatures in atherosclerotic lesions of patients

with coronary heart disease. *Circulation* **113**, 929-937, doi:10.1161/CIRCULATIONAHA.105.579979 (2006).

3 Koren, O. *et al.* Human oral, gut, and plaque microbiota in patients with atherosclerosis. *Proc Natl Acad Sci U S A* **108 Suppl 1**, 4592-4598, doi:10.1073/pnas.1011383107 (2011).

4 Stephen E. Epstein, J. Z., Mary Susan Burnett, Yi Fu Zhou, Gregory Vercellotti, David Hajjar. Infection and Atherosclerosis Potential Roles of Pathogen Burden and Molecular Mimicry. *Arterioscler Thromb Vasc Biol* **20**, doi:10.1161/01.atv.20.6.1417. (2020).

5 Brown, J. M. & Hazen, S. L. The gut microbial endocrine organ: bacterially derived signals driving cardiometabolic diseases. *Annu Rev Med* **66**, 343-359, doi:10.1146/annurev-med-060513-093205 (2015).

6 Bartolomaeus H, B. A., Yakoub M, Homann S, Markó L, Höges S, Tsvetkov D, Krannich A, Wundersitz S, Avery EG, Haase N, Kräker K, Hering L, Maase M, Kusche-Vihrog K, Grandoch M, Fielitz J, Kempa S, Gollasch M, Zhumadilov Z, Kozhakhmetov S. Short-Chain Fatty Acid Propionate Protects From Hypertensive Cardiovascular Damage. *Circulation* **11**, doi:10.1161/CIRCULATIONAHA.118.036652. (2019).

7 Chen, X. F., Chen, X. & Tang, X. Short-chain fatty acid, acylation and cardiovascular diseases. *Clin Sci (Lond)* **134**, 657-676, doi:10.1042/CS20200128 (2020).

8 Xu, Y. *et al.* Hepatocyte ATF3 protects against atherosclerosis by regulating HDL and bile acid metabolism. *Nat Metab* **3**, 59-74, doi:10.1038/s42255-020-00331-1 (2021).

9 Gistera, A. *et al.* Transforming growth factor-beta signaling in T cells promotes stabilization of atherosclerotic plaques through an interleukin-17-dependent pathway. *Sci Transl Med* **5**, 196ra100, doi:10.1126/scitranslmed.3006133 (2013).

10 Wang, Z. *et al.* Non-lethal Inhibition of Gut Microbial Trimethylamine Production for the Treatment of Atherosclerosis. *Cell* **163**, 1585-1595, doi:10.1016/j.cell.2015.11.055 (2015).

11 Karlsson, F. H. *et al.* Symptomatic atherosclerosis is associated with an altered gut metagenome. *Nat Commun* **3**, 1245, doi:10.1038/ncomms2266 (2012).

12 Laman, J. D., Schoneveld, A. H., Moll, F. L., van Meurs, M. & Pasterkamp, G. Significance of peptidoglycan, a proinflammatory bacterial antigen in atherosclerotic arteries and its association with vulnerable plaques. *Am J Cardiol* **90**, 119-123, doi:10.1016/s0002-9149(02)02432-3 (2002).

13 Laman, J. D., t Hart, B. A., Power, C. & Dziarski, R. Bacterial Peptidoglycan as a Driver of Chronic Brain Inflammation. *Trends Mol Med* **26**, 670-682, doi:10.1016/j.molmed.2019.11.006 (2020).

14 Saigusa, R., Winkels, H. & Ley, K. T cell subsets and functions in atherosclerosis. *Nat Rev Cardiol* **17**, 387-401, doi:10.1038/s41569-020-0352-5 (2020).

15 Meng, X. *et al.* Regulatory T cells in cardiovascular diseases. *Nat Rev Cardiol* **13**, 167-179, doi:10.1038/nrcardio.2015.169 (2016).

16 Shohei Hori, T. N., Shimon Sakaguchi. Control of Regulatory T Cell Development by the Transcription Factor Foxp3. *Science* **299** (2003).

17 Kim HJ, B. R., Kreslavsky T, Brown FD, Moffett H, Lemieux ME, Kaygusuz Y, Meissner T, Holderried TA, Chan S, Kastner P, Haining WN, Cantor H. Stable inhibitory activity of regulatory T cells requires the transcription factor Helios. *Science* **350**, 334-339, doi:10.1126/science.aad0616 (2015).

18 Liu, Z. D. *et al.* Increased Th17 cell frequency concomitant with decreased Foxp3+ Treg

cell frequency in the peripheral circulation of patients with carotid artery plaques. *Inflamm Res* **61**, 1155-1165, doi:10.1007/s00011-012-0510-2 (2012).

19 de Boer, O. J., van der Meer, J. J., Teeling, P., van der Loos, C. M. & van der Wal, A. C. Low numbers of FOXP3 positive regulatory T cells are present in all developmental stages of human atherosclerotic lesions. *PLoS One* **2**, e779, doi:10.1371/journal.pone.0000779 (2007).

20 Kim, H. J., Hwang, S. J., Kim, B. K., Jung, K. C. & Chung, D. H. NKT cells play critical roles in the induction of oral tolerance by inducing regulatory T cells producing IL-10 and transforming growth factor beta, and by clonally deleting antigen-specific T cells. *Immunology* **118**, 101-111, doi:10.1111/j.1365-2567.2006.02346.x (2006).

21 Meng, X. *et al.* Regulatory T cells prevent plaque disruption in apolipoprotein E-knockout mice. *Int J Cardiol* **168**, 2684-2692, doi:10.1016/j.ijcard.2013.03.026 (2013).

22 Deaglio, S. *et al.* Adenosine generation catalyzed by CD39 and CD73 expressed on regulatory T cells mediates immune suppression. *J Exp Med* **204**, 1257-1265, doi:10.1084/jem.20062512 (2007).

23 Eid, R. E. *et al.* Interleukin-17 and interferon-gamma are produced concomitantly by human coronary artery-infiltrating T cells and act synergistically on vascular smooth muscle cells. *Circulation* **119**, 1424-1432, doi:10.1161/CIRCULATIONAHA.108.827618 (2009).

24 Smith, E. *et al.* Blockade of interleukin-17A results in reduced atherosclerosis in apolipoprotein E-deficient mice. *Circulation* **121**, 1746-1755, doi:10.1161/CIRCULATIONAHA.109.924886 (2010).

25 Danzaki, K. *et al.* Interleukin-17A deficiency accelerates unstable atherosclerotic plaque formation in apolipoprotein E-deficient mice. *Arterioscler Thromb Vasc Biol* **32**, 273-280, doi:10.1161/ATVBAHA.111.229997 (2012).

26 Madhur, M. S. *et al.* Role of interleukin 17 in inflammation, atherosclerosis, and vascular function in apolipoprotein e-deficient mice. *Arterioscler Thromb Vasc Biol* **31**, 1565-1572, doi:10.1161/ATVBAHA.111.227629 (2011).

27 Valgimigli, M. *et al.* 2017 ESC focused update on dual antiplatelet therapy in coronary artery disease developed in collaboration with EACTS: The Task Force for dual antiplatelet therapy in coronary artery disease of the European Society of Cardiology (ESC) and of the European Association for Cardio-Thoracic Surgery (EACTS). *Eur Heart J* **39**, 213-260, doi:10.1093/eurheartj/ehx419 (2018).

28 Wallentin L, B. R., Budaj A, Cannon CP, Emanuelsson H, Held C, Horrow J, Husted S, James S, Katus H, Mahaffey KW, Scirica BM, Skene A, Steg PG, Storey RF, Harrington RA; PLATO Investigators, Freij A, Thorsén M. Ticagrelor versus Clopidogrel in Patients with Acute Coronary Syndromes. *N Engl J Med* **361**, doi:10.1056/NEJMoa0904327. (2009).

29 Bonaca, M. P. *et al.* Efficacy and Safety of Ticagrelor Over Time in Patients With Prior MI in PEGASUS-TIMI 54. *J Am Coll Cardiol* **70**, 1368-1375, doi:10.1016/j.jacc.2017.07.768 (2017).

30 Verdoia, M., Savonitto, S., Dudek, D., Kedhi, E. & De Luca, G. Ticagrelor as compared to conventional antiplatelet agents in coronary artery disease: A comprehensive meta-analysis of 15 randomized trials. *Vascul Pharmacol* **137**, 106828, doi:10.1016/j.vph.2020.106828 (2021).

31 Storey, R. F. *et al.* Lower mortality following pulmonary adverse events and sepsis with ticagrelor compared to clopidogrel in the PLATO study. *Platelets* **25**, 517-525, doi:10.3109/09537104.2013.842965 (2014).

32 Sexton, T. R. *et al.* Ticagrelor Reduces Thromboinflammatory Markers in Patients With Pneumonia. *JACC Basic Transl Sci* **3**, 435-449, doi:10.1016/j.jacbts.2018.05.005 (2018).

33 Patrizio Lancellotti LM, N. J., et al. . Antibacterial Activity of Ticagrelor in Conventional Antiplatelet Dosages Against Antibiotic-Resistant Gram-Positive Bacteria. *JAMA Cardiology* **4**, doi:10.1001/jamacardio.2019.1189. (2019).

34 He, S. *et al.* Gut intraepithelial T cells calibrate metabolism and accelerate cardiovascular disease. *Nature* **566**, 115-119, doi:10.1038/s41586-018-0849-9 (2019).

35 Brown, E. M., Kenny, D. J. & Xavier, R. J. Gut Microbiota Regulation of T Cells During Inflammation and Autoimmunity. *Annu Rev Immunol* **37**, 599-624, doi:10.1146/annurev-immunol-042718-041841 (2019).

36 Brandsma, E. *et al.* A Proinflammatory Gut Microbiota Increases Systemic Inflammation and Accelerates Atherosclerosis. *Circ Res* **124**, 94-100, doi:10.1161/CIRCRESAHA.118.313234 (2019).

37 Kanthi, Y. *et al.* Flow-dependent expression of ectonucleotide tri(di)phosphohydrolase-1 and suppression of atherosclerosis. *J Clin Invest* **125**, 3027-3036, doi:10.1172/JCI79514 (2015).

38 Wei, J. *et al.* Dietary Polysaccharide from Enteromorpha clathrata Attenuates Obesity and Increases the Intestinal Abundance of Butyrate-Producing Bacterium, Eubacterium xylanophilum, in Mice Fed a High-Fat Diet. *Polymers (Basel)* **13**, doi:10.3390/polym13193286 (2021).

39 Jonsson, A. L. & Backhed, F. Role of gut microbiota in atherosclerosis. *Nat Rev Cardiol* **14**, 79-87, doi:10.1038/nrcardio.2016.183 (2017).

40 Lal, G. *et al.* Distinct inflammatory signals have physiologically divergent effects on epigenetic regulation of Foxp3 expression and Treg function. *Am J Transplant* **11**, 203-214, doi:10.1111/j.1600-6143.2010.03389.x (2011).

41 Park, S. Y., Jing, X., Gupta, D. & Dziarski, R. Peptidoglycan recognition protein 1 enhances experimental asthma by promoting Th2 and Th17 and limiting regulatory T cell and plasmacytoid dendritic cell responses. *J Immunol* **190**, 3480-3492, doi:10.4049/jimmunol.1202675 (2013).

42 Krakauer, T., Pradhan, K. & Stiles, B. G. Staphylococcal Superantigens Spark Host-Mediated Danger Signals. *Front Immunol* **7**, 23, doi:10.3389/fimmu.2016.00023 (2016).

43 Peters, E., Heemskerk, S., Masereeuw, R. & Pickkers, P. Alkaline phosphatase: a possible treatment for sepsis-associated acute kidney injury in critically ill patients. *Am J Kidney Dis* **63**, 1038-1048, doi:10.1053/j.ajkd.2013.11.027 (2014).

44 Ahern, P. P., Faith, J. J. & Gordon, J. I. Mining the human gut microbiota for effector strains that shape the immune system. *Immunity* **40**, 815-823, doi:10.1016/j.immuni.2014.05.012 (2014).

45 Geva-Zatorsky, N. *et al.* Mining the Human Gut Microbiota for Immunomodulatory Organisms. *Cell* **168**, 928-943 e911, doi:10.1016/j.cell.2017.01.022 (2017).

46 Belkaid, Y. & Hand, T. W. Role of the microbiota in immunity and inflammation. *Cell* **157**, 121-141, doi:10.1016/j.cell.2014.03.011 (2014).

47 Clemente, J. C., Manasson, J. & Scher, J. U. The role of the gut microbiome in systemic inflammatory disease. *BMJ* **360**, j5145, doi:10.1136/bmj.j5145 (2018).

48 Pickard, J. M., Zeng, M. Y., Caruso, R. & Nunez, G. Gut microbiota: Role in pathogen colonization, immune responses, and inflammatory disease. *Immunol Rev* **279**, 70-89, doi:10.1111/imr.12567 (2017).

49 Liu, Y. J. *et al.* Parthenolide ameliorates colon inflammation through regulating Treg/Th17 balance in a gut microbiota-dependent manner. *Theranostics* **10**, 5225-5241, doi:10.7150/thno.43716 (2020).

50 Cekanaviciute, E. *et al.* Gut bacteria from multiple sclerosis patients modulate human T cells and exacerbate symptoms in mouse models. *Proc Natl Acad Sci U S A* **114**, 10713-10718, doi:10.1073/pnas.1711235114 (2017).

51 Potekhina, A. V. *et al.* Treg/Th17 balance in stable CAD patients with different stages of coronary atherosclerosis. *Atherosclerosis* **238**, 17-21, doi:10.1016/j.atherosclerosis.2014.10.088 (2015).

52 Nordlohne, J. *et al.* Aggravated Atherosclerosis and Vascular Inflammation With Reduced Kidney Function Depend on Interleukin-17 Receptor A and Are Normalized by Inhibition of Interleukin-17A. *JACC Basic Transl Sci* **3**, 54-66, doi:10.1016/j.jacbts.2017.08.005 (2018).

53 Brauner, S. *et al.* Augmented Th17 differentiation in Trim21 deficiency promotes a stable phenotype of atherosclerotic plaques with high collagen content. *Cardiovasc Res* **114**, 158-167, doi:10.1093/cvr/cvx181 (2018).

54 Hannachi, N. *et al.* Antiplatelet Agents Have a Distinct Efficacy on Platelet Aggregation Induced by Infectious Bacteria. *Front Pharmacol* **11**, 863, doi:10.3389/fphar.2020.00863 (2020).

55 Ulloa, E. R., Uchiyama, S., Gillespie, R., Nizet, V. & Sakoulas, G. Ticagrelor Increases Platelet-Mediated Staphylococcus aureus Killing, Resulting in Clearance of Bacteremia. *J Infect Dis* **224**, 1566-1569, doi:10.1093/infdis/jiab146 (2021).

56 Tatara, A. M., Gandhi, R. G., Mooney, D. J. & Nelson, S. B. Antiplatelet therapy for Staphylococcus aureus bacteremia: Will it stick? *PLoS Pathog* **18**, e1010240, doi:10.1371/journal.ppat.1010240 (2022).

57 Butt, J. H. *et al.* Ticagrelor and the risk of Staphylococcus aureus bacteraemia and other infections. *Eur Heart J Cardiovasc Pharmacother* **8**, 13-19, doi:10.1093/ehjcvp/pvaa099 (2022).

58 Natividad, J. M. *et al.* Bilophila wadsworthia aggravates high fat diet induced metabolic dysfunctions in mice. *Nat Commun* **9**, 2802, doi:10.1038/s41467-018-05249-7 (2018).

59 Huart, J. *et al.* Gut Microbiota and Fecal Levels of Short-Chain Fatty Acids Differ Upon 24-Hour Blood Pressure Levels in Men. *Hypertension* **74**, 1005-1013, doi:10.1161/HYPERTENSIONAHA.118.12588 (2019).

60 Yue, C. *et al.* Medium-, long- and medium-chain-type structured lipids ameliorate high-fat diet-induced atherosclerosis by regulating inflammation, adipogenesis, and gut microbiota in ApoE(-/-) mice. *Food Funct* **11**, 5142-5155, doi:10.1039/d0fo01006e (2020).

61 Song, Y. *et al.* Effects of three different mannans on obesity and gut microbiota in high-fat diet-fed C57BL/6J mice. *Food Funct* **12**, 4606-4620, doi:10.1039/d0fo03331f (2021).

62 Liu, X. *et al.* Blautia-a new functional genus with potential probiotic properties? *Gut Microbes* **13**, 1-21, doi:10.1080/19490976.2021.1875796 (2021).

63 Sun, D. *et al.* Anti-peptidoglycan antibodies and Fcgamma receptors are the key mediators of inflammation in Gram-positive sepsis. *J Immunol* **189**, 2423-2431, doi:10.4049/jimmunol.1201302 (2012).

64 Park, S. Y., Gupta, D., Kim, C. H. & Dziarski, R. Differential effects of peptidoglycan recognition proteins on experimental atopic and contact dermatitis mediated by Treg and Th17 cells. *PLoS One* **6**, e24961, doi:10.1371/journal.pone.0024961 (2011).

65 Josefowicz, S. Z., Lu, L. F. & Rudensky, A. Y. Regulatory T cells: mechanisms of differentiation and function. *Annu Rev Immunol* **30**, 531-564, doi:10.1146/annurev.immunol.25.022106.141623 (2012).

66 Joseph Barbi, D. P., Fan Pan. Treg functional stability and its responsiveness to the microenvironment. *Immunological Reviews* **259**, doi:10.1111/imr.12172. (2014).

67 Wang, E. S. *et al.* Acute pharmacological degradation of Helios destabilizes regulatory T cells. *Nat Chem Biol* **17**, 711-717, doi:10.1038/s41589-021-00802-w (2021).

68 Takatori, H. *et al.* Helios Enhances Treg Cell Function in Cooperation With FoxP3. *Arthritis Rheumatol* **67**, 1491-1502, doi:10.1002/art.39091 (2015).

69 Bedke, T., Muscate, F., Soukou, S., Gagliani, N. & Huber, S. Title: IL-10-producing T cells and their dual functions. *Semin Immunol* **44**, 101335, doi:10.1016/j.smim.2019.101335 (2019).

70 Akhavanpoor, M. *et al.* The Two Faces of Interleukin-17A in Atherosclerosis. *Curr Drug Targets* **18**, 863-873, doi:10.2174/1389450117666161229142155 (2017).

71 Qin, C. *et al.* Critical Role of P2Y12 Receptor in Regulation of Th17 Differentiation and Experimental Autoimmune Encephalomyelitis Pathogenesis. *J Immunol* **199**, 72-81, doi:10.4049/jimmunol.1601549 (2017).

72 Jacob, F., Perez Novo, C., Bachert, C. & Van Crombruggen, K. Purinergic signaling in inflammatory cells: P2 receptor expression, functional effects, and modulation of inflammatory responses. *Purinergic Signal* **9**, 285-306, doi:10.1007/s11302-013-9357-4 (2013).

73 Stachon, P. *et al.* Extracellular ATP Induces Vascular Inflammation and Atherosclerosis via Purinergic Receptor Y2 in Mice. *Arterioscler Thromb Vasc Biol* **36**, 1577-1586, doi:10.1161/ATVBAHA.115.307397 (2016).

74 Buchheiser, A. *et al.* Inactivation of CD73 promotes atherogenesis in apolipoprotein E-deficient mice. *Cardiovasc Res* **92**, 338-347, doi:10.1093/cvr/cvr218 (2011).

75 Allard, B., Beavis, P. A., Darcy, P. K. & Stagg, J. Immunosuppressive activities of adenosine in cancer. *Curr Opin Pharmacol* **29**, 7-16, doi:10.1016/j.coph.2016.04.001 (2016).

76 Reiner, M. F. *et al.* Ticagrelor, but not clopidogrel, reduces arterial thrombosis via endothelial tissue factor suppression. *Cardiovasc Res* **113**, 61-69, doi:10.1093/cvr/cvw233 (2017).

77 Authors/Task Force, m. *et al.* 2014 ESC/EACTS Guidelines on myocardial revascularization: The Task Force on Myocardial Revascularization of the European Society of Cardiology (ESC) and the European Association for Cardio-Thoracic Surgery (EACTS)Developed with the special contribution of the European Association of Percutaneous Cardiovascular Interventions (EAPCI). *Eur Heart J* **35**, 2541-2619, doi:10.1093/eurheartj/ehu278 (2014).

78 Chen, S., Zhou, Y., Chen, Y. & Gu, J. fastp: an ultra-fast all-in-one FASTQ preprocessor. *Bioinformatics* **34**, i884-i890, doi:10.1093/bioinformatics/bty560 (2018).

79 Magoc, T. & Salzberg, S. L. FLASH: fast length adjustment of short reads to improve genome assemblies. *Bioinformatics* **27**, 2957-2963, doi:10.1093/bioinformatics/btr507 (2011).

80 Callahan, B. J. *et al.* DADA2: High-resolution sample inference from Illumina amplicon data. *Nat Methods* **13**, 581-583, doi:10.1038/nmeth.3869 (2016).

81 Davis, S. *et al.* Leveraging crowdsourcing to accelerate global health solutions. *Nat Biotechnol* **37**, 848-850, doi:10.1038/s41587-019-0180-5 (2019).

82 Asshauer, K. P., Wemheuer, B., Daniel, R. & Meinicke, P. Tax4Fun: predicting functional profiles from metagenomic 16S rRNA data. *Bioinformatics* **31**, 2882-2884, doi:10.1093/bioinformatics/btv287 (2015).

83 Li, H. & Durbin, R. Fast and accurate short read alignment with Burrows-Wheeler transform. *Bioinformatics* **25**, 1754-1760, doi:10.1093/bioinformatics/btp324 (2009).

84 Li, D., Liu, C. M., Luo, R., Sadakane, K. & Lam, T. W. MEGAHIT: an ultra-fast single-node solution for large and complex metagenomics assembly via succinct de Bruijn graph. *Bioinformatics* **31**, 1674-1676, doi:10.1093/bioinformatics/btv033 (2015).

85 Buchfink, B., Xie, C. & Huson, D. H. Fast and sensitive protein alignment using DIAMOND. *Nat Methods* **12**, 59-60, doi:10.1038/nmeth.3176 (2015).

917

Table 1| Characteristics of study participants			
	Ticagrelor-aspirin (n=11)	Clopidogrel-aspirin (n=10)	*P* value TAvs CA
Demographics			
Males（n）	6	7	0.659*
Age（years）	59.5±1.6	59.1±1.9	0.89‡
BMI(kg/m^2)		26.7±3.8	0.52‡
Current smoker(n)	2	3	0.635*
Hypertension(n)	7	5	0.67*
Diabetes(n)	5	4	1*
Previous myocardial infarction(n)	0	0	1*
Medication History			
Statin treatment(n)	6	5	1*
Asprin(n)	0	0	1*
Beta blocker treatment(n)	3	2	1*
ACE/ARB treatment(n)	3	2	1*
Antidiabetic(n)	5	4	1*
Laboratory variables			
Cholesterol,(mmol/L)			
Baseline	4.13±0.85	3.69±0.72	0.22‡
On treatment	3.34±0.66	3.58±0.49	0.35‡
Triglycerides,(mmol/L)			
Baseline	2.35±1.4	1.67±0.68	0.18‡
On treatment	1.85±1.02	1.53±0.63	0.4†
HDL-C,(mmol/L)			
Baseline	0.86±1.83	0.92±0.28	0.54‡
On treatment	0.98±0.2	1.08±0.24	0.33‡
LDL-C,(mmol/L)			
Baseline	2.42±0.58	2.17±0.54	0.32‡
On treatment	1.7±0.59	1.97±0.45	0.25‡
WBC(*10^9/L)			
Baseline	6.74±1.92	5.71±1.57	0.2‡
On treatment	6.54±1.29	6.14±1.6	0.53‡
Neutrophil relative value(%)			
Baseline	64.71±10.83	57.69±6.82	0.11‡
On treatment	59.87±8.72	58.81±5.77	0.75‡
Lymphocyte relative value(%)			
Baseline	25.85±7.26	30.79±6.36	0.12‡
On treatment	31.01±6.75	28.68±5.92	0.45‡

*Fisher's exact test.‡Welch's t-test. BMI=body mass index; ACE=angiotensin-converting enzyme; ARB= angiotensin receptor blocker; HDL=high-density lipoprotein; LDL= low-density lipoprotein

918

919 **Table1 Characteristics of study participants.**

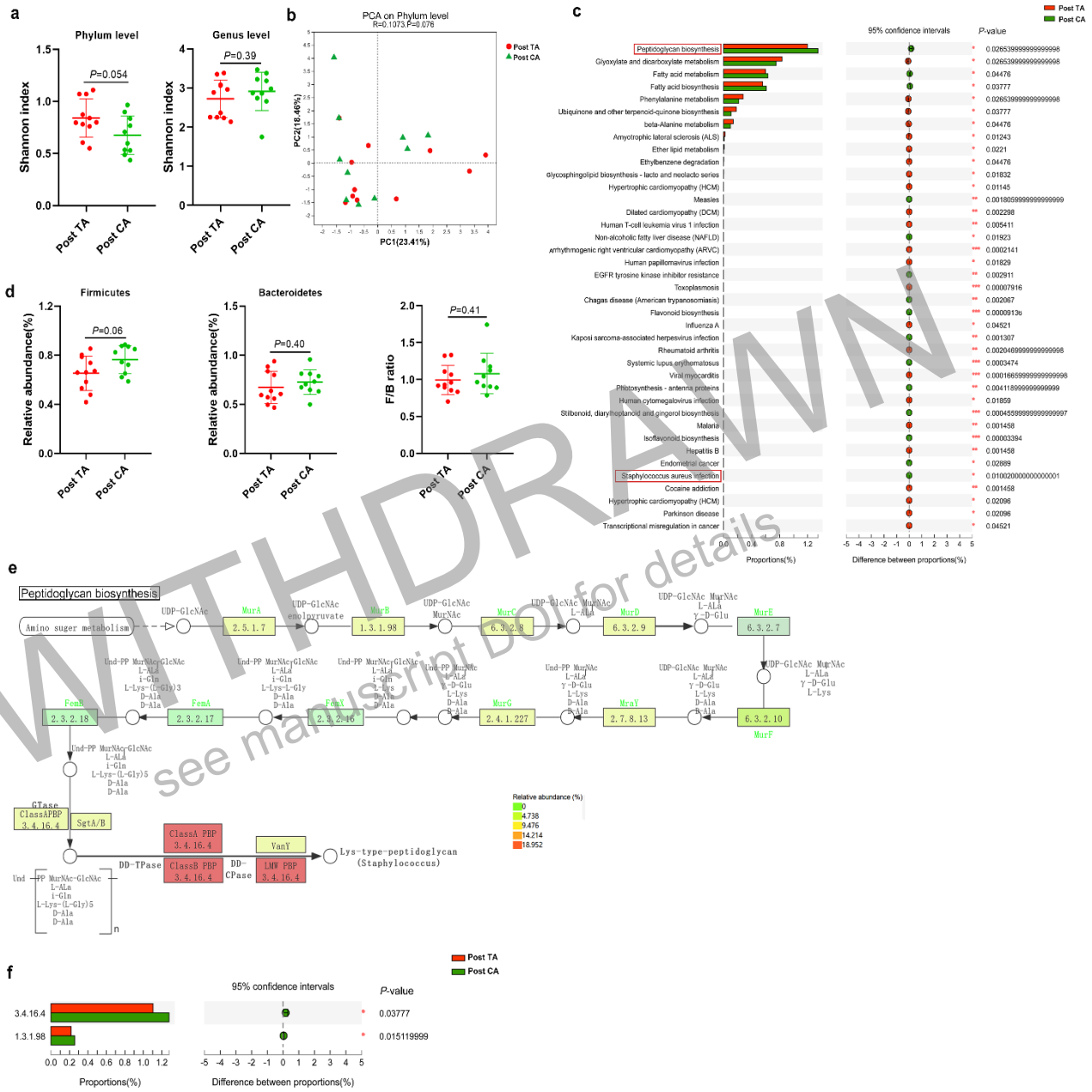

Figure 1. Distinct gut microbial composition and function under the one-month treatments of ticagrelor-aspirin and clopidogrel-aspirin in individuals with UAP. Shannon index at the phylum and genus levels by 16S rRNA (**a**). Principal coordinate analysis (PCA) at the phylum level was performed based on Bray-curtis (**b**). Relative abundance of *Firmicutes* and *Bacteroidetes* at the phylum level, and the *Firmicutes to Bacteroidetes* (*F/B*) ratio by 16S rRNA (**c**). Kyoto Encyclopedia of Genes and Genomes (KEGG) pathways generated from the metagenomic analysis based on the reads number relative (**d**). Expression of enzymes involved in PGN biosynthesis based on the KEGG

Orthology database (**e**). Proportions of two enzymes that had statistical differences involved in PGN biosynthesis (**f**). The 2-tailed Student's t-test was used to detect significant difference between two groups (**a-e**). Data were expressed as mean±SEM (**a, b**). PGN biosynthesis pathway map (map00550) is cited from http://www.kegg.jp/kegg/kegg1.html with permission. PGN: peptidoglycan. Post TA: Post ticagrelor-aspirin. Post CA: Post clopidogrel-aspirin.

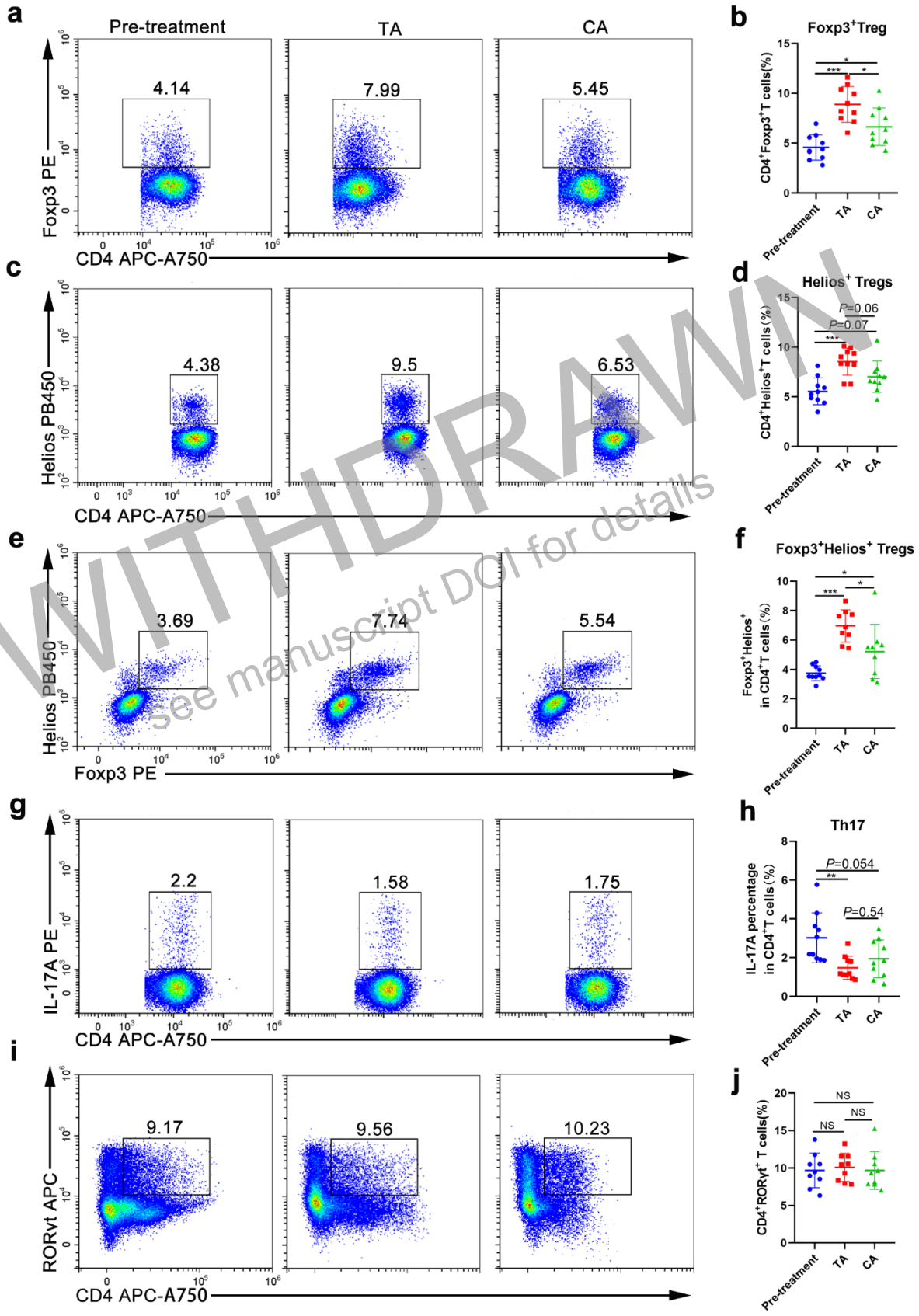

Figure 2. Ticagrelor-aspirin increased the Tregs but not Th17 cells compared to clopidogrel-aspirin. Representative flow cytometry plots and quantifications of

regulatory T cells and Th17 cells in the PBMC from individuals of pre-treatment, TA, and CA groups (**a-j**). Representative flow cytometry plots (**a**, **c**, **e**) and quantifications (**b**, **d**, **f**) of $Foxp3^+$, $Helios^+$, and $Foxp3^+Helios^+$ Tregs respectively within the $CD4^+$ population. Representative flow cytometry plots (**g**, **i**) and quantifications (**h**, **j**) of $ROR\gamma t^+$ and $IL\text{-}17A^+$ Th17 respectively within the $CD4^+$ population. Each symbol represents an individual in diverse group. Data were shown as mean ± SEM and were analyzed by one-way ANOVA followed by a *post hoc* Tukey's test. TA: ticagrelor-aspirin, CA: clopidogrel-aspirin, PBMC: Peripheral blood mononuclear cells, Foxp3: Forkhead box protein P3, a transcription factor of Treg, Helios: a transcription factor of Tregs, RORγt: RAR-related orphan receptor γt, a transcription factor of Th17. IL-17A: interleukin 17A. $^*P<0.05$, $^{**}P<0.01$, $^{***}P<0.001$

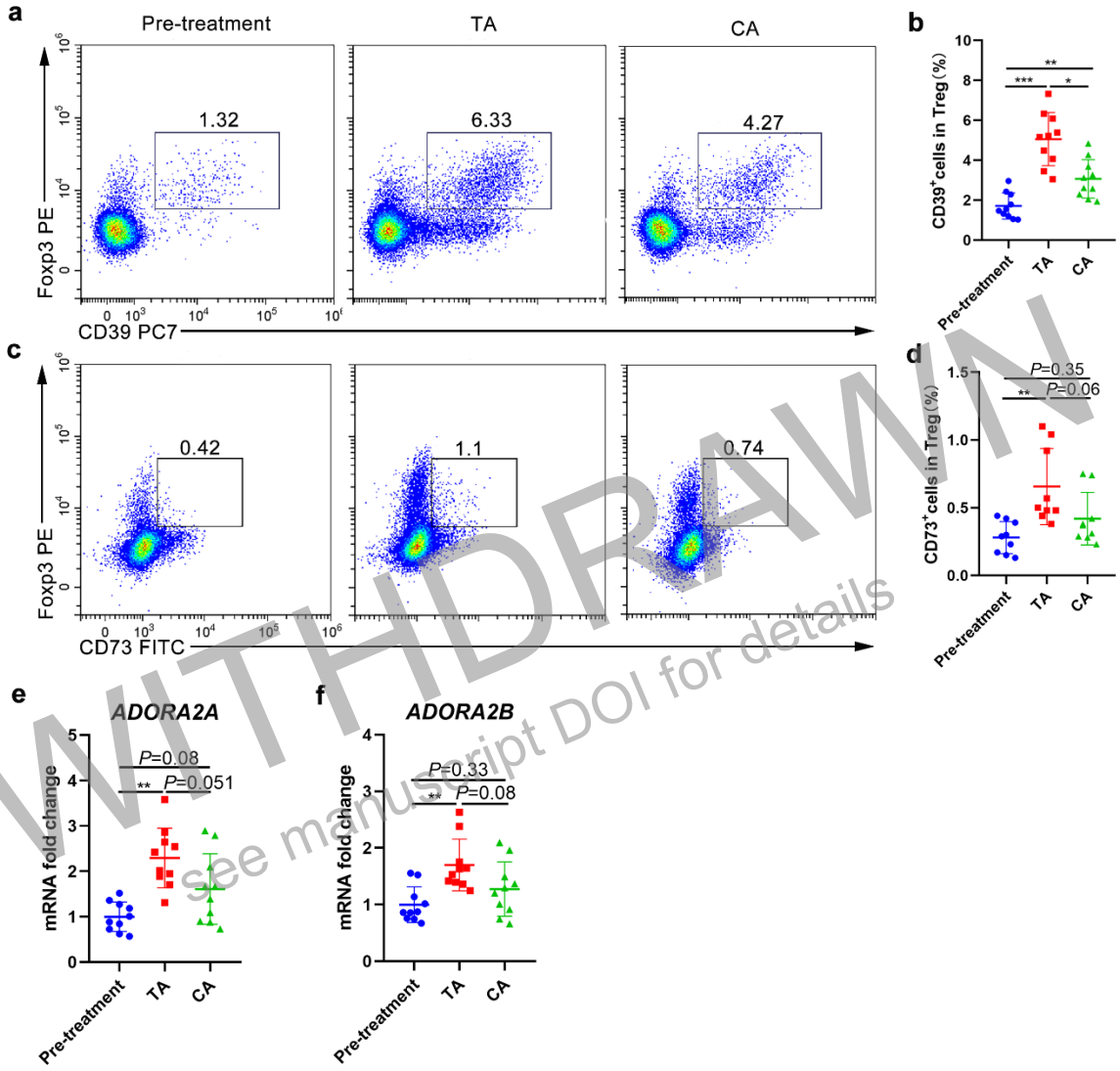

Figure 3. Ticagrelor-aspirin induced higher CD39/CD73 expression on Tregs mediated partially the anti-inflammatory effect in human. Representative flow cytometry plots (**a**, **c**) and quantifications (**b**, **d**) of $CD39^{+}Foxp3^{+}$ and $CD73^{+}Foxp3^{+}$cells within the $CD4^{+}$ populations. The gene expressions *ADORA2A* and *ADORA2B* in PBMC were analyzed by qPCR and normalized to *β-ACTIN* (**e**, **f**). Each symbol represents an individual in diverse group. TA: ticagrelor-aspirin, CA: clopidogrel-aspirin. Data were shown as mean ± SEM and were analyzed by one-way ANOVA followed by a *post hoc* Tukey's test. ADORA2A: adenosine receptor A2A. ADORA2B: adenosine receptor A2B. $^{*}P<0.05$, $^{**}P<0.01$, $^{***}P<0.001$

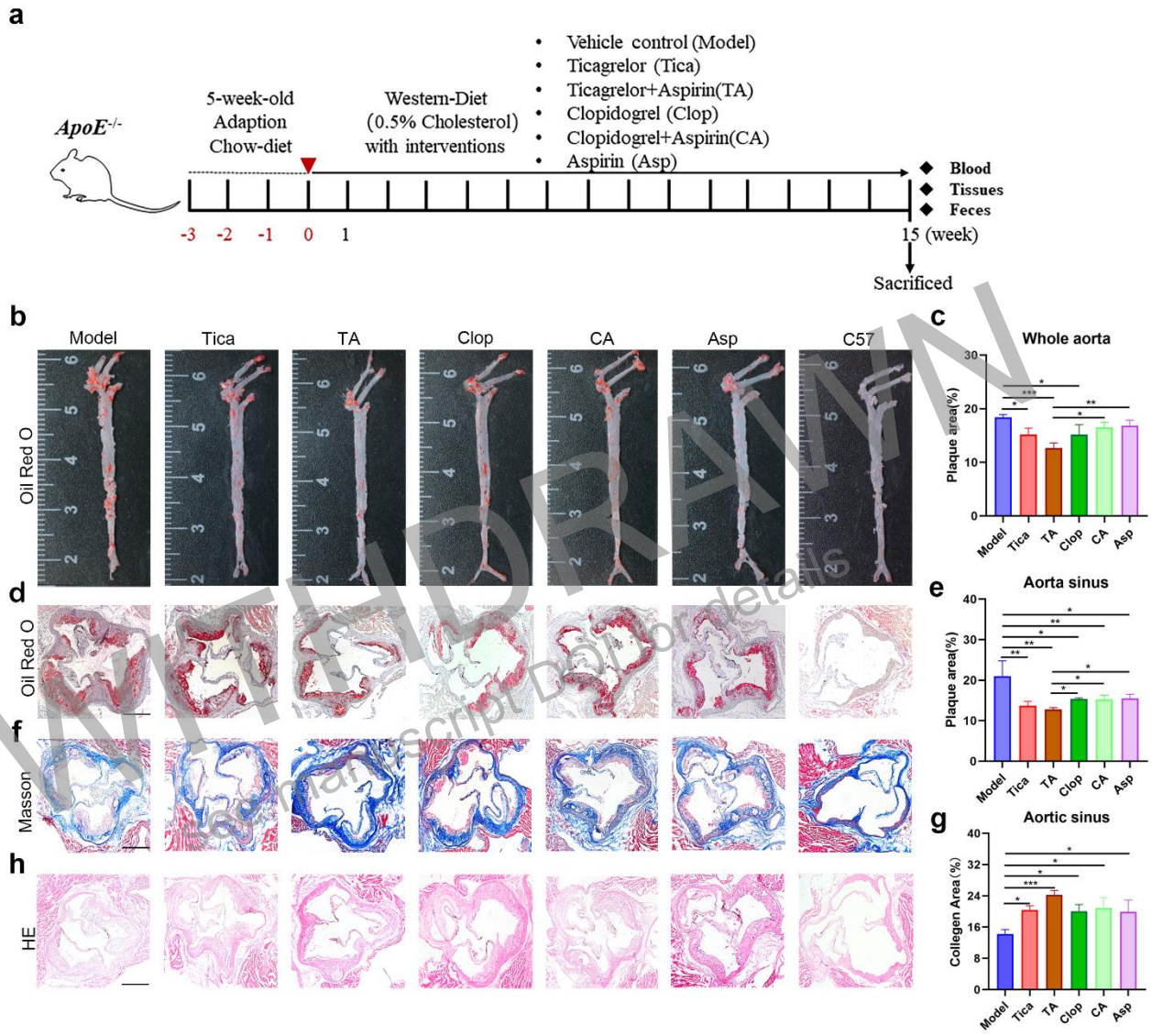

Figure 4. Effects of different antiplatelet medications' treatments limited plaque progression in atherosclerotic *ApoE*$^{-/-}$ mice. Schematic diagram of diverse treatments in *ApoE*$^{-/-}$mice (**a**). Representative of Oil Red O in the whole aorta and aorta sinus (**b**, **d**). Quantifications of Oil Red O in the whole aorta and aorta sinus (**c**, **e**). Representative and quantification of Masson staining in aorta sinus (**f**, **g**). Representative histological H&E section of the aorta sinus (**h**). Scar bar, 200 μm. Tica: ticagrelor. TA: ticagrelor+aspirin. Clop: clopidogrel. CA: clopidogrel+aspirin. Asp: aspirin. Data were shown as mean ± SEM and were analyzed by one-way ANOVA followed by a *post hoc* Tukey's test. $^{*}P<0.05$, $^{**}P<0.01$, $^{***}P<0.001$

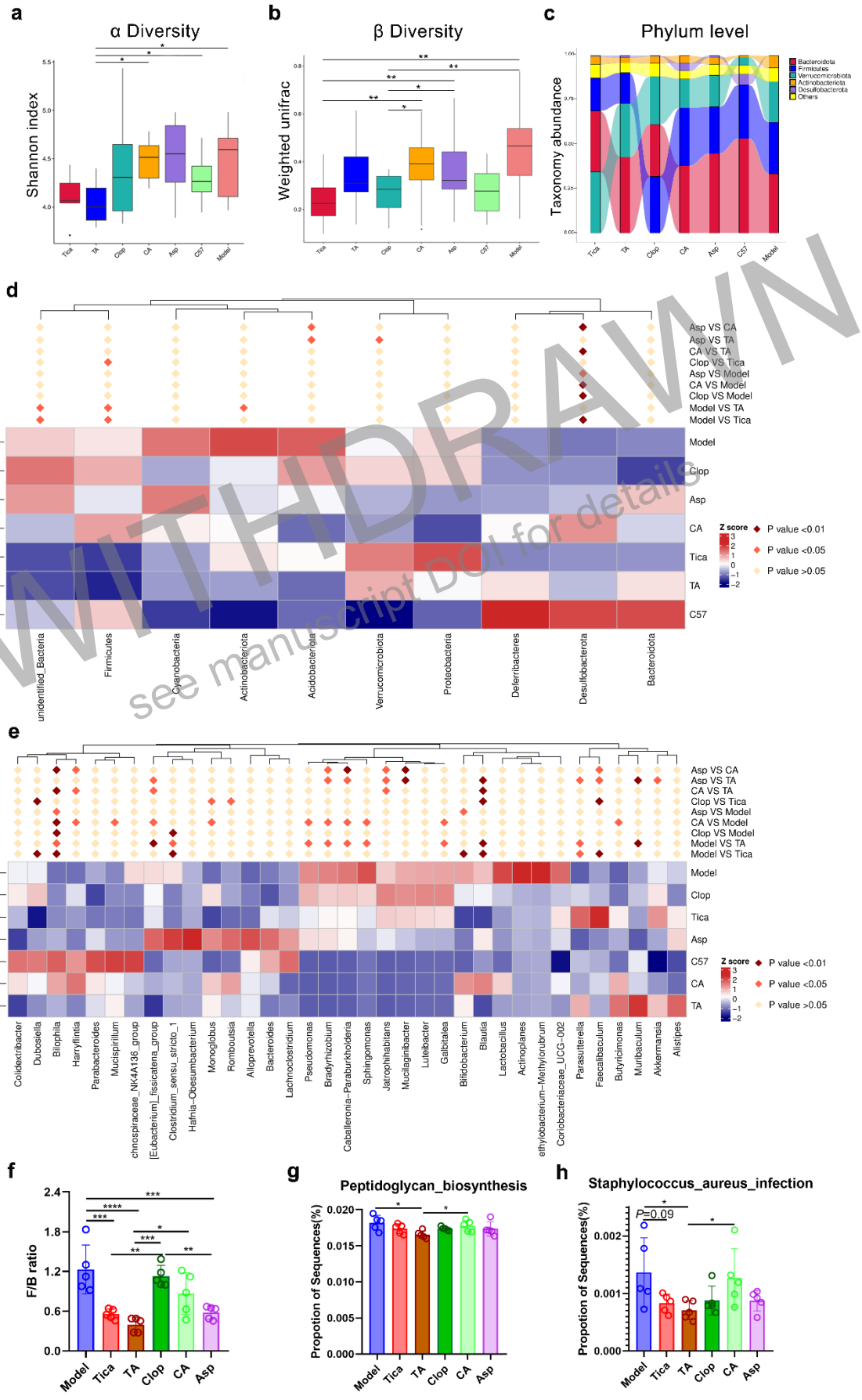

972

Figure 5. Ticagrelor and Ticagrelor-aspirin regulated the gut microbiota to a "healthier" state in atherosclerotic *ApoE*$^{-/-}$ mice. α diversity of Shannon index (**a**) and β diversity by weighted unifrac (**b**). Relative abundance of taxa at the phylum level (**c**). Matastat analysis of the relative proportion of taxa at the phylum level (**d**) and genus level (**e**). *Firmicutes to Bacteroidetes* (*F/B*) ratio (**f**). PGN and *S. aureus* infection pathways were predicted by Tax4fun of 16S rRNA sequencing data (**g**, **h**). PGN: peptidoglycan. *S. aureus*: *staphylococcus aureus.* Tica: ticagrelor. TA: ticagrelor+aspirin. Clop: clopidogrel. CA: clopidogrel+aspirin. Asp: aspirin. Data were shown as mean ± SEM and were analyzed by one-way ANOVA followed by a *post hoc* Tukey's test. $^{*}P<0.05$, $^{**}P<0.01$, $^{***}P<0.001$.

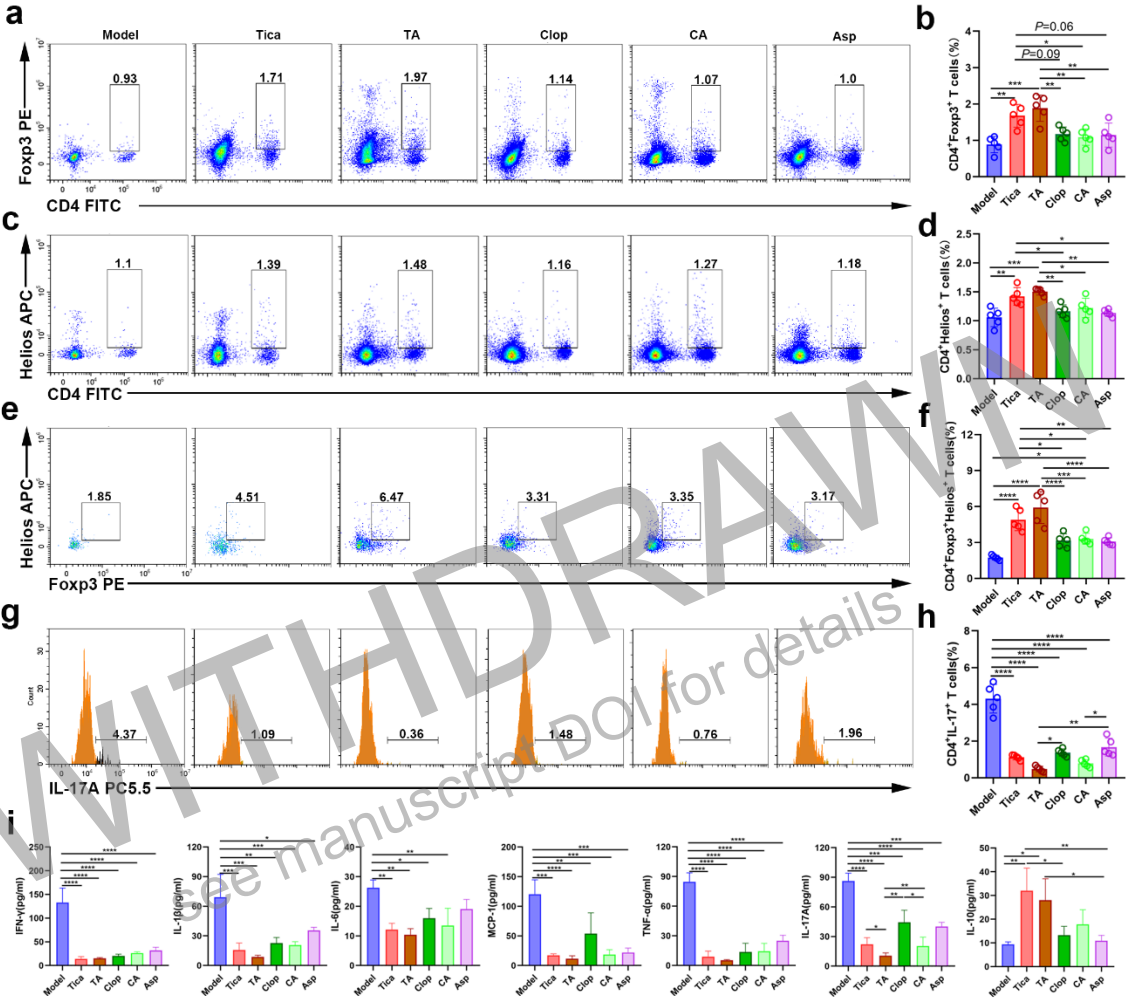

Figure 6. Ticagrelor-aspirin exerted optimal synergistic effects among all the antiplatelet medicine in balancing the Treg/Th17 axis and anti-inflammatory profile in atherosclerotic *ApoE*$^{-/-}$ mice. Representative flow cytometry plots (**a**, **c**, **e**) and quantifications (**b**, **d**, **f**) of Foxp3$^+$, Helios$^+$, and Foxp3$^+$Helios$^+$ Tregs respectively within the CD4$^+$ population in blood. Representative flow cytometry plots (**g**) and quantifications (**h**) of IL-17A$^+$ Th17 within the CD4$^+$ population in blood. Inflammatory cytokines (IFN-γ, IL-1β, IL-6, MCP-1, TNF-α, IL-17A, and IL-10) were detected and quantified in plasma (**i**). Tica: ticagrelor. TA: ticagrelor+aspirin. Clop: clopidogrel. CA: clopidogrel+aspirin. Asp: aspirin. Data were shown as mean ± SEM and were analyzed by one-way ANOVA followed by a *post hoc* Tukey's test. $^*P<0.05$, $^{**}P<0.01$, $^{***}P<0.001$, $^{****}P<0.0001$.

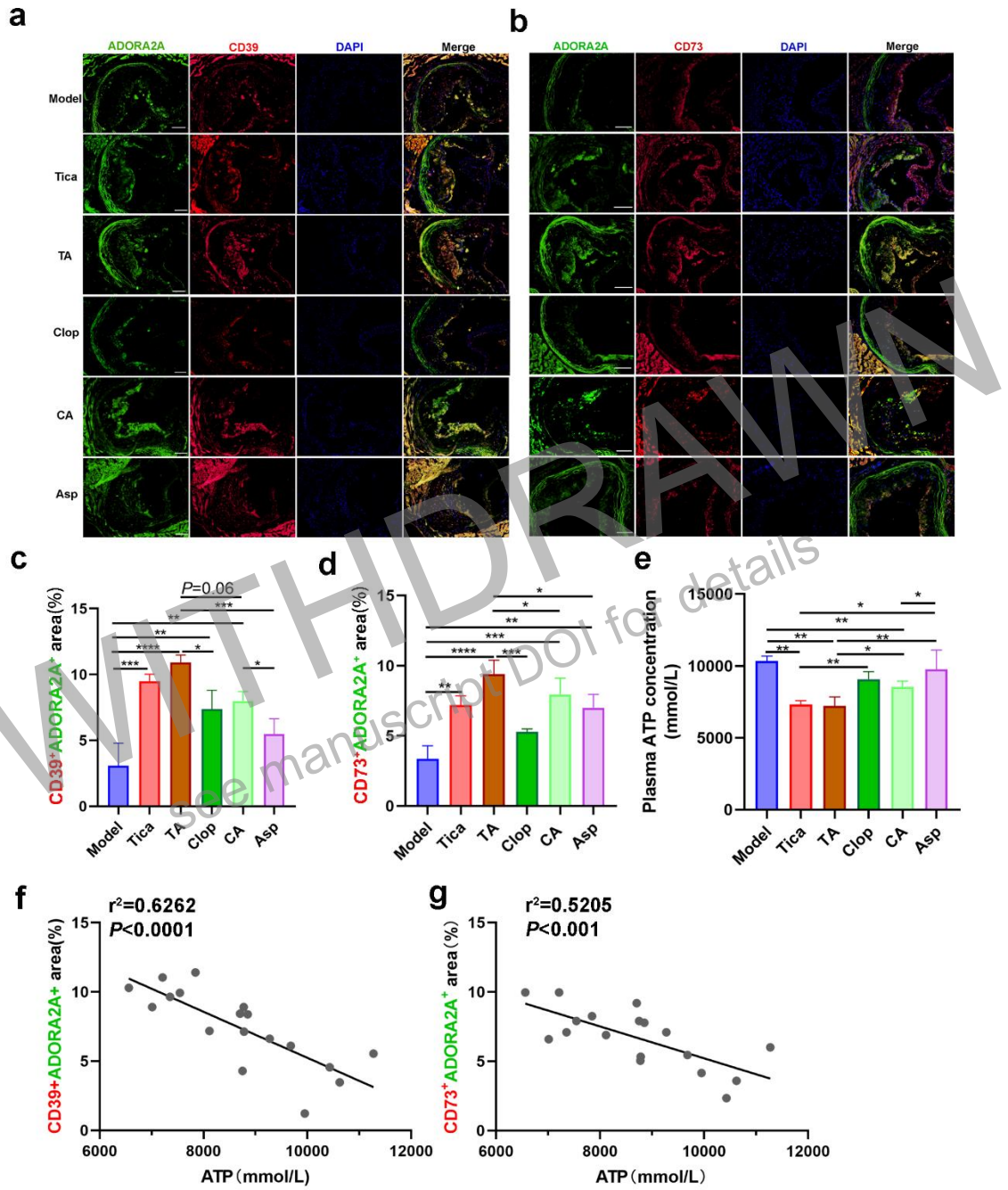

Figure 7. Expression and relationship among the CD39, CD73, ADORA2A and ATP among diverse groups in atherosclerotic *ApoE*$^{-/-}$ mice. Representative fluorescence images of CD39 (red) with ADORA2A (green) in aortic root lesions from *ApoE*$^{-/-}$mice in diverse groups (**a**). Nuclei were stained with DAPI (blue). Graph showed the number of CD39^{+} ADORA2A^{+} cells in indicated groups (**c**). Representative fluorescence images of CD73 (red) with ADORA2A (green) in aortic root lesions from *ApoE*$^{-/-}$mice in diverse groups (**b**). Nuclei were stained with DAPI (blue). Graph

showed the number of $CD73^+$ $ADORA2A^+$ cells in indicated groups (**d**). Analysis of the concentration of circulating ATP from *ApoE*$^{-/-}$mice (**e**). Analysis of the correlation between the concentration of circulating ATP and the number of $CD39^+$ $ADORA2A^+$ (**f**), $CD73^+$ $ADORA2A^+$ (**g**) cells in the atherosclerotic plaques of aortic sinuses from *ApoE*$^{-/-}$mice on different treatments. Scale bar, 40 μm. Tica: ticagrelor. TA: ticagrelor+aspirin. Clop: clopidogrel. CA: clopidogrel+aspirin. Asp: aspirin. ADORA2A: adenosine receptor A2A. DAPI: 4′,6-diamidino-2-phenylindole. Data were shown as mean ± SEM and were analyzed by one-way ANOVA followed by a *post hoc* Tukey's test. $^{*}P<0.05$, $^{**}P<0.01$, $^{***}P<0.001$, $^{****}P<0.0001$.

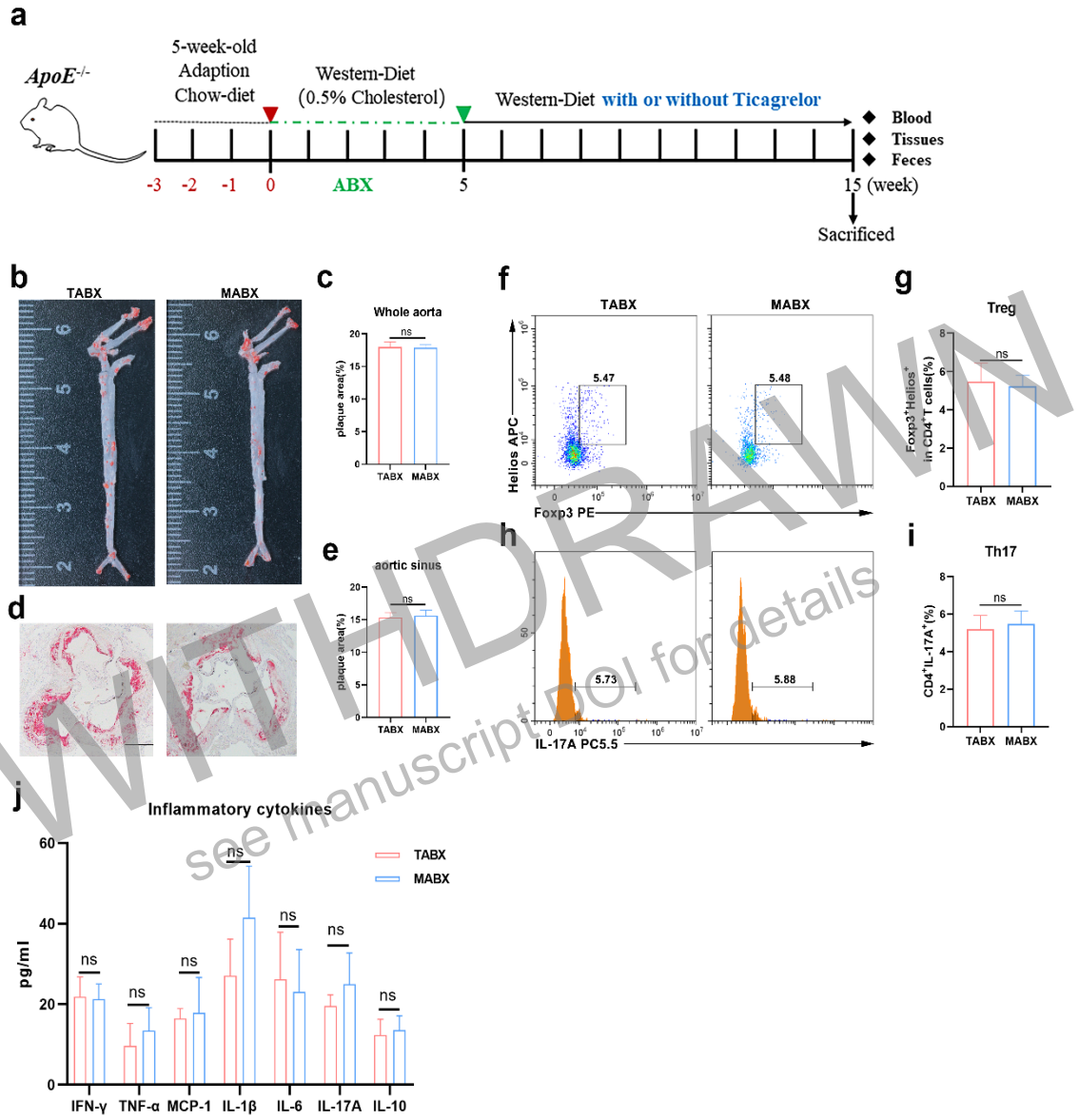

Figure 8 Effects of Tica on plaque area, circulatory Treg/Th17 cells and inflammatory cytokines of *ApoE*$^{-/-}$ mice after removed microbiota by ABX. Schematic diagram of ABX experiment **(a).** Representative of Oil Red O in the whole aorta and aorta sinus (**b, d**). quantifications of Oil Red O in the whole aorta and aorta sinus (**c, e**). Representative flow cytometry plots (**f, h**) and quantifications (**g, i**) of Foxp3^{+}Helios^{+} Tregs and IL-17A^{+} Th17 respectively within the CD4^{+} population in blood. Concentration of inflammatory cytokine in plasma between the two groups (**j**). n=5 per each group. Scar bar, 200 μm. TABX: ticagrelor-ABX, MABX: Model-ABX. Data were shown as mean ± SEM and were analyzed by the Student' t-test.